The Thesis Committee for Elizabeth Ann Brown
Certifies that this is the approved version of the following thesis:

Defining the metabolic compensation pathways employed during low-level hypercapnia in red drum (*Sciaenops ocellatus*)

APPROVED BY
SUPERVISING COMMITTEE:

Supervisor:

Andrew Esbaugh

Peter Thomas

Benjamin Walther

Defining the metabolic compensation pathways employed during low-level hypercapnia in red drum (*Sciaenops ocellatus*)

by

Elizabeth Ann Brown, B.S.

Thesis

Presented to the Faculty of the Graduate School of

The University of Texas at Austin

in Partial Fulfillment

of the Requirements

for the Degree of

Master of Science in Marine Science

The University of Texas at Austin

August 2015

Dedication

This work is dedicated to my family, whose overwhelming support has been a constant source of inspiration throughout this endeavor. I would especially like to dedicate this to my parents who have fostered my love of science and the sea for longer than I can remember and have always encouraged me to get the best education I could possibly get; my brother, Alex, who spent countless hours of our vacations with me combing across beaches looking for sea life and who taught me that a good dose of sibling rivalry can be the best motivation in the world; and my fiancé, Tommy, who has stood by me and willingly gone along with all of my academic aspirations. Lastly, I would like to dedicate this work to my Oma, who first took me to Sea World and sparked my love of the ocean. I believe that if she were here, she would get great joy from this.

Acknowledgements

I would not have been able to complete this work without the endless, unwavering love and support of my family: my mom, who has always been an inimitable source of advice and encouragement; my dad, who taught me to find value in everything (especially failed experiments and negative results); my step-mom, who spent many late nights with me discussing ideas and results; my brother and partner-in-crime, who has understood and mirrored my excitement for marine science for as long as I can remember; and my fiancé, who has been constant and irreplaceable source of inspiration and morale throughout these scientific endeavors. I would like to thank Jeff Kaiser at the Fisheries and Mariculture Labs for his invaluable advice on red drum care and maintenance. My lab mates – the A-Team – Dr. Rasmus Ern and Joshua Lonthair for assisting with many aspects of this work as well as providing me with daily doses of laughter and sarcasm. Venus Mills, Erin Frolli, Matt Seeley and everyone at FAML and MSI for acting as sounding boards and keepers of my sanity when data analysis got difficult. I would like to thank my committee members Dr. Peter Thomas and Dr. Ben Walther for their many suggestions, helpful edits, and constructive feedback throughout the course of this work. Finally, I'd like to extend my innumerable thanks to my supervisor, Dr. Andrew Esbaugh, whose continual thoughts on this project allowed to evolve into its final form. This work could not have been accomplished without any of them.

Abstract

Defining the metabolic compensation pathways employed during low-level hypercapnia in red drum (*Sciaenops ocellatus*)

Elizabeth Ann Brown, M.S.Marine.Sci.
The University of Texas at Austin, 2015

Supervisor: Andrew Esbaugh

Since the pre-industrial era, anthropogenic CO_2 emissions have raised oceanic CO_2 by 40% and reduced ocean pH by 0.1 unit. This results in acid-base disturbances in marine organisms that are compensated through regulatory pathways. Many estuarine fishes, including red drum (*Sciaenops ocellatus*), regularly encounter periods of elevated CO_2, which may impart a level of species resilience to ocean acidification. Initial studies examined the time course of whole animal acid-base compensation in response to varying CO_2 concentrations. Under control conditions red drum showed net base excretion; however, the onset of CO_2 exposures resulted in a dose-dependent increase in acid excretion during the initial 2h time period. Notably, net acid excretion returned to baseline levels by 4h of exposure of up to 5,000 μatm, but remained elevated throughout 15,000 and 30,000 μatm exposures. Subsequent studies assessed the plasticity of branchial acid-base pathways after exposure to various CO_2 levels using qPCR. 1,000 μatm exposed fish were sampled at 1h, 4h, 24h, 72h, and 14d, while 6,000 and 30,000 μatm exposed fish were

sampled after 1h, 4h, and 24h of exposure. Of a suite of acid-base relevant genes, only the Na^+ HCO_3^- co-transporter (NBC) was upregulated in 1,000 and 6,000 μatm treatments. In contrast, the majority of relevant genes were up-regulated by 4h of exposure to 30,000 μatm, with the exception of the electrogenic anion exchanger slc26a3a, which was only upregulated by 24h of exposure to 30,000 μatm. Cytoplasmic carbonic anhydrase and Na^+ H^+ exchanger 1 exhibited no change in expression to 30,000 μatm. Localization studies examined the position of the V-type H^+ ATPase (VHA) within gill ionocytes. Under control conditions, VHA is diffusely distributed throughout the cytoplasm of the cell, although oriented toward the apical pole; there was no evidence of basolateral localization. Exposure to 6,000 μatm CO_2 did not result in translocation of cytoplasmic VHA to the apical membrane. Overall, these results indicate that red drum can quickly compensate to a wide range of environmentally relevant acid-base disturbances using baseline cellular machinery, yet are capable of acid-base plasticity in response to extreme challenges.

Table of Contents

List of Tables

List of Figures

Introduction

Acid-base balance is a fundamental physiological process for all organisms. Fundamentally, acid-base balance is the sum of physiological processes that act to maintain plasma and tissue pH in the face of environmental or metabolic challenges. These challenges can be described as either an alkalosis or an acidosis, depending on whether pH increases or decreases. A number of different stresses can lead to pH fluctuations, including exercise, digestion and osmoregulation. These are all examples of a metabolic disturbance whereby the pH change is the result of shifts in plasma HCO_3^-. While these types of disturbances are common to all vertebrates, fishes are particularly susceptible to a second form of disturbance – a respiratory disturbance. A respiratory disturbance occurs when the partial pressure of CO_2 in the blood is altered causing a cascade of chemical changes culminating in a pH change. The most common such disturbance is a respiratory acidosis caused by elevated aquatic CO_2. Recent work has shown that a respiratory acidosis can be caused by increases of as small as 0.06% CO_2 in the environment (Esbaugh et al. 2012). This has generated renewed interest in acid-base balance in the context of ocean acidification and climate change, as well as the numerous examples of localized low level hypercapnia found globally. Not surprisingly, fishes are well adapted to compensate for respiratory acidoses. In particular, gills contain a large abundance of ionocytes, which are cells specialized for the transport of ions and acid-base equivalents (Perry and Gilmour 2006; Claiborne et al. 2002; Marshall and Grosell 2005). This literature review will discuss the particular proteins that are associated with marine ionocytes with specific emphasis on their roles in acid-base balance.

It is theorized that marine teleosts use a suite of regulatory genes – Na^+/H^+ exchangers, V-type H^+ ATPase, Na^+/HCO_3^- co-transporters, carbonic anhydrases, and members of the slc26 gene family – to compensate for the physiological challenges induced by acid-base disturbances. These genes may be up- or down-regulated in response to external environmental conditions (Claiborne et al. 1999; Mount and Romero 2004; Grosell and Genz 2006; Ivanis et al. 2008; Bayaa et al. 2009; Parks et al. 2008; Guffey et al. 2011; Hu et al. 2013; Liu et al. 2013; Roa et al. 2014). The ability of teleosts to exhibit phenotypic plasticity and regulate the expression of these genes may be critical to their ability to compensate for acid-base disturbances induced by environmental stresses that result in an acidosis.

Acid excreting ionocytes (Figure 1) play an important role in preventing blood acidoses by transporting H^+ into the environment. One family of genes that has been shown to regulate the movement of acid across the respiratory epithelia is the Na^+/H^+ exchangers (NHE). Early work on NHEs focused on their role in ionoregulatory pathways; however, studies have shown that they also function in acid-base regulatory capacities (Claiborne et al. 1999; Hu et al. 2013; Liu et al. 2013). NHEs are members of the slc9 gene family, and while they all function as proton exchangers, they are differentially located throughout the cell and can be independently regulated depending on internal and external environmental conditions (Orlowski and Grinstein 2004). Freshwater teleosts utilize both NHEs and V-type ATPases (VHA) to apically excrete protons into the environment (Figure 1). However, Claiborne et al. (2002) have suggested that marine teleosts may use NHEs to excrete protons when presented with an acidosis (J. B. Claiborne et al. 2002). The NHE-1

protein functions as a "housekeeping" protein in the basolateral membrane of the marine gill ionocyte, as well as most cells of the body, and functions to protect intracellular acid-base status. In the gill, this protein is down-regulated during a respiratory acidosis (Claiborne et al. 1999), which acts to protect plasma pH. NHE-2 and NHE-3 have both been localized to the apical membrane of ionocytes in marine and freshwater gills (Ivanis et al. 2008; Liu et al. 2013). While experiencing hypercapnia induced respiratory acidosis, both marine and freshwater NHE-2 was up-regulated, implicating its role as an acid-base regulatory protein (Evans et al. 2005; Ivanis et al. 2008).

Carbonic anhydrase (CA) is another protein that is tightly connected to H^+ excretion. Its role in the cell is to catalyze the hydration of CO_2 into H^+ and HCO_3^-, thus providing the substrate for acid and base excretion (Haswell et al. 1980; Goss et al. 1998; Georgalis, Gilmour, et al. 2006; Georgalis, Perry, et al. 2006; Gilmour and Perry 2009). This process creates a portion of the H^+ and HCO_3^- that is transported across the respiratory epithelia during acid-base regulation (Grosell and Genz 2006; Perry et al. 2009). The Na^+/HCO_3^- co-transporter (NBC) has also been implicated as a regulatory gene in the acid-base regulating pathway (Figure 1). NBC has been suggested to transport HCO_3^- across the basolateral epithelia in both marine and freshwater fishes (Parks et al. 2008; Perry et al. 2010; Guffey et al. 2011; Heuer et al. 2012). In *Opsanus beta*, a euryhaline marine species, NBC up-regulation was observed in the gill following transfer to hypersalinity (Taylor et al. 2010). It is assumed that this up-regulation is in response to the correlated acidosis and that NBC may play a compensatory role by increasing the movement of HCO_3^-

across the basolateral membrane (Guffey et al. 2011; Esbaugh et al. 2012), thus defending against the plasma acidosis.

The ability to buffer against an acidosis by up-taking HCO_3^- from the environment is a potentially important route to compensation. The slc26 gene family codes for a variety of genes involved in exchanging HCO_3^- and Cl^- ions (Bayaa et al. 2009; Mount and Romero 2004; Parks et al. 2009). Two members of this family code for proteins that are stoichiometrically opposite of each other; slc26a3 is a protein that facilitates the exchange of 2 Cl^- ions for 1 HCO_3^- ion. Slc26a6, conversely, exchanges 1 Cl^- ion for 2 HCO_3^- ions (Mount and Romero 2004). Slc26a3 was originally identified in mammals as a possible tumor suppressor and may play a weak role in regulation of cell growth (Mount and Romero 2004). In teleosts, slc26a3 is commonly found in the gills and plays an important role in Cl^- uptake in fresh water, as the most significant of the slc26 genes for Cl^- entry into ionocytes under normal conditions (Bayaa et al. 2009). In marine fishes, the movement of Cl^- out of the cell against an electrochemical gradient for HCO_3^- from the environment via slc26a3 may be a useful pathway for providing the necessary base equivalents to buffer against an acidosis.

Slc26a6 is one of the most widely expressed members of the slc26 gene family, and it has been most commonly observed via immunohistochemistry on the apical membranes of epithelial tissues (Mount and Romero 2004). In freshwater teleosts, slc26a6 plays a role in Cl^- uptake similar, although to a lesser extent, to slc26a3 (Bayaa et al. 2009; Grosell, Mager, et al. 2009). Movement of acid-base equivalents through these slc26 proteins is not electroneutral and require a depolarization event for slc26a3 and a hyperpolarization

for slc26a6 to function (Mount and Romero 2004). Individually, these pathways would be thermodynamically unfavorable for HCO_3^- uptake from the environment. However, it is hypothesized that if slc26a3 is localized in cells that contain Na^+ K^+ $2Cl^-$ co-transporters (NKCC), the electrochemical gradient that allows for Cl^- excretion through the CFTR channel could make a HCO_3^- uptake pathway more favorable (Figure 2). In fact, this pathway could conceivably be energetically favorable to NHE as it utilizes electrochemical gradients that must already be generated for general osmoregulatory pathways.

Effects of CO_2 dose on H^+ excretion pathways in red drum (*Sciaenops ocellatus*) gills

INTRODUCTION

Anthropogenic CO_2 emissions have been rising rapidly since the industrial revolution causing an increase in atmospheric CO_2. This CO_2 dissolves into oceanic surface waters, where it reacts with water to form bicarbonate (HCO_3^-) and protons (H^+). Since the pre-industrial era, oceanic CO_2 levels have risen by as much as 30% raising the CO_2 partial pressure (pCO_2) to 400 μatm, which has caused the pH of ocean water to drop by 0.1 units (Raven et al. 2005; Caldeira 2005; Orr et al. 2005; Caldeira and Wickett 2003; Meehl et al. 2007). Estimates suggest that if current trends continue, oceanic pCO_2 could reach 1,000 μatm by the end of the century, reducing surface water pH by 0.3-0.4 units (Raven et al. 2005; Caldeira 2005; Orr et al. 2005).

Ocean acidification has been shown to have numerous behavioral and ecological effects on marine fishes (Ishimatsu et al. 2008; Munday et al. 2010; Munday et al. 2009; Simpson et al. 2011; Dixson et al. 2010; Cripps et al. 2011; Nilsson et al. 2012; Ferrari et al. 2012). It is thought that these effects are the consequence of elevated blood HCO_3^- that is the result of compensation to a respiratory acidosis (Esbaugh et al. 2012; Strobel et al. 2012). It is generally accepted that marine fishes compensate for a respiratory acidosis by transporting acid and base equivalents into the environment and plasma, respectively, through specialized gill ionocytes. Apical transport of protons is thought to primarily occur through NHE2 and NHE3 (Claiborne et al. 2008; J. B. Claiborne et al. 2002; Claiborne et al. 1999; Edwards et al. 2001; Edwards et al. 2005; Guffey et al. 2015). This pathway is

particularly effective for marine fishes owing to the steep inward Na^+ gradient. Protons are produced from CO_2 by cytoplasmic carbonic anhydrase (CA-c; (Esbaugh et al. 2005)), which also produces HCO_3^-. This HCO_3^- is transported back into the plasma by the electrogenic Na^+ HCO_3^- co-transporter (Perry and Gilmour 2006), which has the benefit of raising plasma HCO_3^- thereby offsetting the increase in plasma CO_2 and returning pH to basal values. More recently, studies have highlighted the importance of V-type ATPase translocation in compensating for alkalosis (Roa et al. 2014; Tresguerres et al. 2007(a)). It is as yet unclear if similar translocation to the apical membrane may play a role in compensating for an acidosis.

The resilience of marine fish species to the long-term environmental degradation caused by ocean acidification is dependent on a number of factors. While evolutionary adaptation to ocean acidification is a possible route for some fishes with short generation times, typical evolutionary processes are thought to be too slow to provide a tangible route to resilience for long lived species (Pfister et al. 2014). Instead, a major factor is thought to be the presence of resilient genotypes that may already exist within a species or population (Gonzalez et al. 2013; Pfister et al. 2014). A second major factor is the phenotypic plasticity of a species, either within an individual or through transgenerational mechanisms, as this is hypothesized to extend the time for more standard evolutionary processes to occur (Pfister et al. 2014; Esbaugh et al. 2012; Heuer et al. 2012). Due to clear implications of ocean acidification for fish acid-base balance, understanding the baseline capacity and plasticity of acid-base pathways is particularly relevant.

Estuarine fishes potentially act as ecologically and environmentally relevant models for the study of the impacts of ocean acidification and other low level acid-base disturbances. Estuaries play important roles in the life cycles of many marine teleost species by providing shelter and food to larval and juvenile individuals. Additionally, the biogeochemical aspects of estuaries makes them susceptible to changes driven by ocean acidification (Feely et al. 2010; Cai et al. 2011). Conversely, the regular diel shifts of CO_2 in estuaries may provide fishes that inhabit these areas with a degree of built in resilience to acid-base disturbances. Red drum (*Sciaenops ocellatus*) utilize estuaries extensively during their lifecycle (Matlock 1987; Rooker & Holt 1997; Stunz et al. 2002) and can potentially act as model species to determine the physiological mechanism employed by marine teleosts to compensate for hypercapnia driven acid-base disturbances. As such, this study aimed to characterize the physiological response of red drum to varying levels of respiratory acidosis. The first objective was to characterize the time course of whole animal acid excretion in response to increasing acidosis severity. A second objective was to assess the short-term and long-term physiological plasticity in response to both environmentally relevant and physiologically extreme scenarios.

METHODS

Animal Handling

Sub-adult red drum were collected from Texas Parks and Wildlife hatchery in Corpus Christi, Texas, or spawned and raised at the University of Texas Marine Science Institute Fisheries and Mariculture Laboratories, Port Aransas, Texas. Fish were housed

in recirculating systems with UV treated natural seawater collected from the Port Aransas ship channel. All tanks were aerated and ammonia was controlled by circulating water through a biofilter. Temperature was controlled using automated in-line heater/chiller units. CO_2 was kept low through regular partial water replacement using ancillary flow-through lines. All fish were held on a 14 h: 10 h light dark cycle. Fish were fed daily with commercially available Aquamax pelleted dry food and fish were acclimated to control conditions in the facility for at least two weeks prior to experimentation. All experiments were conducted in accordance with protocols approved the University of Texas at Austin Institutional Animal Care and Use Committee.

Whole Animal Acid Flux Methods

Sub-adult red drum (n = 30, mean ± S.E.M = 14.5± 0.7g) were starved for 24 hours prior to and throughout the experiment. Fish were placed in individual chambers (approximately 365 mL) with flow-through control seawater (salinity 32, temperature 22ºC, pH 8.12) and aeration. All individuals underwent an 8 hour acclimation period prior to experimentation. After the acclimation period, the water source was removed and individuals underwent a 16 hour control period in which basal acid flux was measured, followed by a one hour flush period prior to initiating hypercapnia exposures.

Hypercapnia exposures were initiated by removing the water source and switching aeration from ambient room air to room air mixed with nominal 1,000, 2,000, 5,000, 15,000, or 30,000 μatm CO_2. For all flux periods, water samples were taken at the beginning and end of the flux period for determination of titratable alkalinity and ammonia.

The exact time of each sampling point was noted and pH was measured at the onset of each flux period to verify CO_2 treatment levels. pH, temperature, titratable alkalinity and salinity measurements were also taken from the flush reservoir. At the conclusion of control and hypercapnia flux periods the individual chambers with water were weighed and the weight of the fish and empty chamber was subtracted to obtain the flux chamber volume. Known sample volume was added to the calculated flux chamber volume where appropriate.

Immediately following water sample collection, each 25 mL flux period water sample was aerated with pure N_2 gas for 15 minutes to remove any contribution of respiratory CO_2 from the sample. Samples collected to verify CO_2 treatment levels did not undergo N_2 aeration. 10 mL of each sample was then titrated at room temperature with 0.1 N HCl using an automated Apollo SciTech AS-ALK2 alkalinity titrator and accompanying software to determine titratable alkalinity. Ammonia concentrations were measured in each sample using a standard colorimetric assay (Verdouw et al. 1978). Amiloride inhibition experiments were performed as above with the exception that experimental chambers were inoculated with 1 mM amiloride or 0.1% DMSO vehicle at the onset of hypercapnia exposure. Initial water samples were taken 15 min after drug inoculation and flux periods consisted of a single 6 h interval at 30,000 μatm CO_2.

CO_2 Exposure

Sub adult red drum were held in 300 L recirculating tanks supplied with filtered, UV treated Port Aransas ship channel water (pH = 8.15) for at least two weeks prior to CO_2

exposure. Fish were then transferred into a 300 L exposure tank or a 300 L control tank. Food was withheld for at least 24 hours prior to sampling. Initial experiments were performed at control, 6,000 μatm, and 30,000 μatm nominal CO_2 for 4h and 24h (n= 8/ treatment, mean body weight ± S.E.M = 39.5± 5.8g). Gill samples exposed to 1,000 μatm nominal CO_2 for 4h, 24h, 72h, and 14d with concurrent controls were obtained from a previous data set (Esbaugh et al. In Review). Additional 1h exposures were run at 1,000 μatm and 6,000 μatm nominal CO_2 with concurrent controls (n = 8/ treatment, mean ± S.E.M = 32.7± 1.5g). Each level of hypercapnia was maintained by aerating tanks through a gas-water equilibration tower with CO_2 controlled with gas mass flow controllers, control tanks were aerated with ambient room air. pCO_2 exposure levels were calculated using CO_2 Calc software (Robbins et al., 2010) using pH and titratable alkalinity measurements. Immediately following exposure, specimens were euthanized with an overdose of tricane methanesulfonate (MS 222; 250 mg/l buffered with 500 mg/l $NaHCO_3$) followed by spinal transection. Gill tissue samples were collected from each specimen, placed in RNALater, and subsequently stored at -80°C until processing. A second gill sample was collected from control and 1h exposed fish and fixed in z-fix (Anatech Ltd.) overnight then stored in 70% ethanol until processing.

Molecular Methods

Real time PCR primers were developed for NBC and VHA, whereas primers for NHE-1, NHE-2, NHE-3, CAc and elongation factor 1α (EF1-α) had previously been developed for red drum (Watson et al. 2014). Full length sequences for both NBC and

VHA were identified from an in-house gill/intestine transcriptome using Blaststation software. The identified sequences were then verified against the NCBI database using a standard Blast search. Primer pairs were identified using Primer3Plus software package (Untergasser et al., 2007). All primers and GenBank accession numbers for related sequences can be found in Table 1.

Gill lamellae stored in RNALater were washed twice in 500 µL PBS before homogenization. Total RNA isolation was performed using TriReagent according to manufacturer protocols. Concentration and purity of total RNA was measured using a NanoDrop ND-1000 spectrophotometer (Thermo Scientific). Total RNA was treated for potential DNA contamination by incubating with DNase 1 (Thermo Scientific), according to manufacturer protocols. cDNA synthesis was performed on 1 µg of total RNA using RevertAid M-Mulv reverse transcriptase (Thermo Scientific), according to manufacturer protocols. For all cDNA synthesis runs no reverse transcriptase controls was performed to test for genomic DNA contamination. Samples were then diluted 10-fold using nuclease free water and stored at -20°C until qPCR analysis.

qPCR analysis was performed using the Maxima SYBR Green kit (Thermo Scientific). Reactions were prepared according to the manufacturer's protocols with the exception that a 12.5 µl total reaction volume was used. All reactions were processed using an MX3000P qPCR machine (Stratagene) with accompanying software. A serial dilution was used for standard curves to determine the reaction efficiency of each primer pair. For all genes, negative and no reverse-transcriptase control reactions were performed. The CT values for each sample were used to assess relative abundance of each gene in relation to

the control gene elongation factor 1α (EF1-α) using the delta-delta CT method (Pfaffl 2004).

Immunohistochemistry Methods

Prior to staining, samples were dehydrated by three washes with 95% ethanol for 60 minutes followed by three washes with 100% ethanol for 45 minutes followed by a 1h butanol wash and an overnight soak in butanol. Samples were then washed twice for 90 minutes in Histochoice clearing agent. Two paraplast washes were then conducted at 58°C for 1h before samples were set in paraffin and allowed to harden at room temperature. Samples were then stored at 4°C until sectioning. Samples were sectioned at 20 μm and mounted onto Superfrost Plus slides where they were rehydrated, deparaffinised and soaked in DI water until ready to stain. Each slide contained at least two sections so that no primary antibody controls could be run concurrently with each sample. Prior to staining an antigen recovery procedure was performed by heating slides in boiling 10mM Citrate buffer solution three times for 5 minutes. Hydrophobic barriers were drawn around each sample and samples were washed in blocking buffer (PBST with 5% fetal calf serum) twice for 5 minutes. Samples were then incubated with primary antibodies for NKA [1:100] and VHA [1:200] at 4°C overnight. The primary polyclonal rabbit antibody for NKA (sc-28800) was obtained from the Santa Cruz Biotechnology and has been previously verified for fish (Riou et al. 2012; Sucré et al. 2010). The primary monoclonal mouse antibody for VHA was obtained from Santa Cruz Biotechnology and its presence in the gill was confirmed with a Western Blot that produced only a single band of approximately 50 kDa

(data not shown). The VHA antibody epitope (Santa Cruz Biotechnology) also exhibits 97% homology to the red drum VHA sequence found in an in-house red drum gill/ intestine transcriptome. Following primary incubation samples were washed in blocking buffer three times for 5 minutes then incubated with secondary antibodies – goat anti-rabbit Alex Flour 555 [1:500] and goat anti-mouse Alexa Flour 488 [1:500] (Life Technologies) – in the dark for 1 h. Samples were then washed with blocking buffer three times for 5 minutes and mounted using Vectorshield with DAPI. Finally, samples were stained with Sudan Black for 20 minutes and washed in PBS for 10 minutes and stored in dark at 4°C until imaged.

Statistical Methods

All gene expression data for CO_2 treatments were assessed by ANOVA against control groups with the exception of the 1h exposure to 6,000 μatm and 1,000 μatm CO_2 series which had concurrently run control groups for all time points and thus were assessed by Student's *t*-test. All statistical tests were performed with a fiducial level of significance of $P < 0.05$.

Dose-response data were analyzed using one way repeated measures ANOVAs to detect changes in H^+ excretion during CO_2 exposure relative to the 16-hour control period. Changes in H^+ excretion during the amiloride exposure – against controls and between treatments – were analyzed using a two-way ANOVA.

RESULTS

Acid Flux

Dose-response to CO_2

During the 16 h control period, all doses except the 5,000 µatm dose exhibited negative H^+ excretion – as indicated by negative H^+ excretion under control conditions (Figure 3). The 5,000 µatm dose exhibited a slight acid excretion but was not significantly different than zero (one sample t-test). All doses of CO_2 significantly increased H^+ excretion by 2 h post exposure. H^+ excretion in the 1,000 µatm dose was significantly increased at all time points compared to the control period; however, excretion was not significantly different than zero at any time point (one sample t-test). The 2,000 µatm and 5,000 µatm CO_2 doses returned to control excretion rates by 4 h post exposure. In both the 15,000 µatm and 30,000 µatm CO_2 doses, H^+ excretion remained elevated throughout the time series, although in both cases excretion rates appeared to be returning to control levels.

Amiloride Exposure

Red Drum again exhibited HCO_3^- excretion during the 16 h control period prior to inoculation with amiloride or DMSO (mean ± S.E.M. = -0.17 ± 0.07). There was no significant effect of 1 mM amiloride (mean ± S.E.M. = 1.35 ± 0.11) versus DMSO controls (mean ± S.E.M. = 1.38 ± 0.08).

Gene Expression

Exposure to 1,000 µatm nominal CO_2 induced changes in only two genes during the initial 24 h exposure. NBC was transiently upregulated at 4h of exposure followed by a slight, but significant, downregulation at 24 h. NHE-1 was also significantly downregulated at 24 h post-exposure (Figure 4). No changes were observed in expression of NHE-2, NHE-3, or VHA during the 1,000 µatm CO_2 exposure. No changes in expression were observed during the initial 4 h of exposure to 6,000 µatm CO_2 exposure, although NBC was significantly upregulated at 24 h (Figure 5). In contrast, the 30,000 µatm CO_2 exposure induced significant upregulation of NHE-2, NHE-3, NBC, and VHA as early as 4 h post-exposure, all of which remained elevated at 24h exposure. No changes were observed in expression of NHE-1 or CAc (Figure 6).

Due to the lack of responses at 1,000 and 6,000 µatm CO_2, a second series of experiments were performed to specifically assess earlier responses that may occur during the active H^+ excretion period. A 1 h exposure time point was chosen based on the significantly elevated acid excretion shown for this time interval above (Figure 3). Surprisingly, the only observed expression changes were a down-regulation for CAc in both exposures, as well as a down-regulation of NHE-2 in the 6,000 µatm CO_2 exposure (Figure 7).

A final experiment assessed potential plasticity in response to more prolonged exposure to ocean acidification (1,000 µatm CO_2); however, there was no significant effect at either 72 h or 14 d post-exposure (Figure 8).

Immunohistochemistry

Immunohistochemical analysis of red drum gills verified that VHA was most abundantly expressed in ionocytes, as identified by co-localization with NKA (Figure 9). Note that VHA antibody specificity was verified using Western blots, which revealed a single 55 kDa band (data not shown). While VHA and NKA were co-localized to the same cells, they were not found in the same part of the cell as evidenced by the lack of overlapping fluorescence – as indicated by a yellow color. Three dimension reconstruction suggests that VHA localization is mostly cytoplasmic, although come apical expression is possible (Figure 10). No evidence of basolateral VHA localization was observed. To investigate the role of possible translocation to the apical membrane in compensation from an acidosis fish were exposed to 6,000 μatm CO_2 for 1 h, after which VHA localization was again assessed. However, there was no evidence of translocation of VHA to the apical membrane (Figure 10)

DISCUSSION

My results largely support the conventional models with respect to marine acid-base balance in fish, and furthermore clearly demonstrate that red drum are quite effective at dealing with environmentally relevant acid-base disturbances ($\leq$ 6,000 μatm CO_2). While some degree of plasticity was observed in the acid excretion machinery of red drum, even at acid-base disturbances as low as 1,000 μatm, these events typically took place after the animal's acid excretion rates had returned to control levels, suggesting this may be a defensive response to protect against potentially greater acid-base stresses. These results

are not entirely surprising as sub-adult red drum are estuarine-dependent, and therefore can routinely encounter diel shifts in environmental CO_2 and pH levels.

During the acid flux experiment, the rate of H^+ excretion by red drum appeared to increase sequentially with increased CO_2 partial pressure. Red drum responded quickly to a respiratory acidosis as the first 2 h of exposure appear to exhibit the highest rates of H^+ excretion. This is not surprising as previous work on a variety of marine species has shown similar patterns (Edwards et al. 2001; Edwards et al. 2005; Claiborne et al. 2008). After the 2 h time point, the three lowest doses (1,000, 2,000, and 5,000 µatm CO_2) had all returned to zero or control levels where they remained for the duration of the trial. Interestingly, the excretion rates between the 15,000 and 30,000 µatm doses at 2 hours of exposure are similar. This could implicate a maximum excretion rate near 4 µmol g^{-1} h^{-1}. Both the 15,000 and 30,000 µatm CO_2 treatments remained elevated relative to the control period throughout the time trial; however they both exhibit a time-dependent trend of decreasing excretion rates towards control levels. Interestingly, the continued acid excretion suggests that the systemic acid-base disturbance was not fully compensated during the 2-4 h and 4-6 h intervals, yet the observed excretion rates were below maximum. This might be related to a thermodynamic constraint caused by the increased plasma HCO_3^- most likely owing to basolateral HCO_3^- transport from the ionocytes. Nonetheless, these trends suggest that even at high levels of hypercapnia, red drum are able to efficiently compensate for an acidosis.

To more fully verify the predominant role of NHE proteins in net acid excretion, we attempted to inhibit acid excretion using the well-known NHE inhibitor, amiloride.

Surprisingly, inoculation with amiloride had no significant impact on net H^+ excretion rates of red drum exposed to 30,000 μatm CO_2. This is in contrast to experiments run on freshwater teleosts where amiloride successfully inhibited the H^+ excretion pathways (primarily NHE's) in the gills (Kumai and Perry 2011). While it could be interpreted that these results suggest NHE is not a predominant route for apical H^+ transport, I believe this to be unlikely. A more plausible explanation is that seawater may reduce the effectiveness of amiloride, either through reduced solubility or competition with Na^+ (Benos 1982). While increasing the concentration of amiloride within the experimental chambers may have had more success in inhibiting H^+ excretion, amiloride becomes non-specific at higher concentrations – lessening the ability to accurately determine the source of excretion inhibition.

The relatively few changes in gene expression found in the 1,000 μatm and 6,000 μatm CO_2 exposures provide further evidence that red drum have adequate machinery in place to compensate for environmentally relevant acid-base disturbances. Of the genes tested, only NBC showed a response at both CO_2 levels. This may indicate that NBC is the limiting step in the compensation pathways. The slight downregulation of NBC that occurred at 24 h in the 1,000 μatm CO_2 treatment could be a secondary response after protein levels had been elevated. . The other notable response was an observed down-regulation of NHE-1 at 24 h of exposure to 6,000 μatm CO_2. It is well-known that NHE-1 is found on the basolateral membrane where it acts to move protect intracellular pH by moving H^+ from the cell into the plasma (Orlowski & Grinstein 2004; Claiborne et al.

1999). NHE-1 down-regulation would therefore be expected to reduce H^+ transport into the blood further helping to maintain systemic acid-base balance in the face of an acidosis.

It is somewhat surprising that neither NHE-2 nor NHE-3 showed any up-regulation when exposed to 1,000 or 6,000 μatm CO_2, as these two proteins are thought to be crucial in acid-base compensation (Edwards et al. 2005; Claiborne et al. 1999; Ivanis et al. 2008; Claiborne et al. 2002). In fact, the only response was a transient down-regulation of NHE-2 at the 1 h time point in 6,000 μatm. This is likely the result of high enough baseline activity to account for these acid-base disturbances, which is supported by the whole animal acid flux measurements discussed above. Interestingly, a previous study showed that red drum NHE-2 and NHE-3 expression was also unchanged in the gill in response to freshwater transfer (Watson et al. 2014). It is well-known that NHE proteins play a major role in Na^+ uptake in freshwater and many euryhaline species show significant up-regulation in response to freshwater transfer (Gilmour et al. 2012; Edwards et al. 2005; Scott et al. 2005; Reilly et al. 2011). The fact that red drum do not show up-regulation to this osmoregulatory stress – presumably a stress that would require more consistent NHE function than under seawater conditions – is further evidence that these animals may simply maintain high NHE proteins levels in their gills under normal circumstances. Nonetheless, the proof of principle 30,000 μatm CO_2 treatment indicated that NHE-2 and -3 – as well as NBC and VHA – are capable of plasticity in response to an acidosis.

Another noteworthy finding from the 30,000 μatm CO_2 treatment was the significant up-regulation of VHA. While the involvement of VHA in freshwater acid-base compensation is well established (Goss et al. 1998; Lin et al. 1994), this role is less certain

for marine fishes. To date, most of the work examining VHA in marine acid-base compensation has focused on the translocation of cytoplasmic proteins to the basolateral membrane of ionocytes in response to an alkalosis (Roa et al. 2014; Tresguerres et al. 2007(a); Tresguerres et al. 2007(b)). However, it is important to note that this has not been demonstrated for a marine teleost. The current results suggest that VHA may play a role in H^+ excretion across the apical membrane in marine fishes. VHA is strongly co-localized with NKA in the red drum gills, which is somewhat different from previous results with longhorn sculpin that showed expression both in NKA rich and ionocytes and a second non-NKA expressing cell population (Catches et al. 2006). However, the localization of VHA within the cell does not provide much functional insight as the protein is found largely in the cytoplasmic fraction, although it appears to be oriented toward the apical pole. Unlike previous work on alkalosis, there was no evidence of translocation of VHA to the apical membrane during hypercapnia at 6,000 μatm. This lack of migration agrees with the lack of VHA gene expression changes at low levels, but does not account for the rapid H^+ excretion observed during the first 2 h of hypercapnia exposure. While these results provide some support for the potential involvement of VHA in defending an acidosis, the lack of translocation suggests that either VHA is not involved under environmentally realistic scenarios, or that no recruitment of additional VHA activity is necessary. Further work should examine whether VHA translocation may occur under more severe acid-base disturbances.

A final interesting finding was the consistent down-regulation of CA-c during the critical initial 2 h of exposure. This was surprising as the function of cytoplasmic CA in

the gills of marine fishes should be in an acid-base capacity. Unlike in freshwater fishes, branchial CA is not required in an osmoregulatory capacity in marine fishes. However, previous work on the gulf toadfish (*Opsanus beta*), another estuarine species, showed results similar to ours during a 1,900 μatm exposure series (Esbaugh et al., 2012). Those authors speculated this response may be related to the up-regulation of a transepithelial HCO_3^- uptake pathway, which was supported by the inability of toadfish to properly defend the acidosis when HCO_3^- was removed from the exposure medium. Cytoplasmic CA activity may be a detriment to such a pathway as it would potentially dehydrate HCO_3^- upon uptake.

In conclusion the combination of the whole animal acid flux, gene expression and immunohistochemistry provides an interesting and thorough description of how red drum are able to compensate for hypercapnia induced acid-base disturbances. It appears that red drum maintain high levels of baseline machinery to compensate for environmentally relevant pCO_2 levels – up to at least 6,000 μatm. This likely stems from their estuarine habitat where a number of factors can contribute to large shifts in ambient CO_2 levels. While these results largely conform to the accepted models of marine acid-base regulation, they have also provided new evidence for a role of VHA in defending acid-base disturbances, at least under extreme conditions, as well as provided tentative support – through CAc down-regulation – for a possible role for transepithelial HCO_3^-. However, further work is clearly required to more fully elucidate the contribution of these novel pathways of acid-base compensation.

Potential role of slc26 HCO_3^- transporters in acidosis compensation in red drum (*Sciaenops ocellatus*)

INTRODUCTION

Since the pre-industrial era, anthropogenic CO_2 emissions have been rising rapidly, causing a shift in the oceanic carbonate system – raising pCO_2 levels to 400 μatm and dropping the pH by 0.1 unit. If left unaltered, pCO_2 levels will reach 1,000 μatm and oceanic pH will drop by 0.3-0.4 units by the end of the century (Caldeira and Wickett 2003; Caldeira 2005; Meehl et al. 2007; Orr et al. 2005; Raven et al. 2005). This changing environment presents challenges to marine fishes, specifically maintaining internal acid-base balance when hypercapnic waters induce an acidosis (Esbaugh et al. 2012; Strobel et al. 2012). Estuarine fishes potentially act as ecologically and environmentally relevant models for the study of the impacts of ocean acidification and other low level acid-base disturbances. Estuaries play important roles in the life cycles of many marine teleost species – acting as nurseries as well as providing shelter and food to larval and juvenile individuals. Additionally, the biogeochemical aspect of estuaries makes them susceptible to changes driven by ocean acidification (Feely et al. 2010; Cai et al. 2011). Conversely, the regular diel shifts of CO_2 in estuaries may provide fish that inhabit these areas with a degree of built in resilience to acid-base disturbances. Red drum (*Sciaenops ocellatus*) utilize estuaries extensively during their lifecycle and can potentially act as model species to determine the physiological mechanism employed by marine teleosts to compensate for hypercapnia driven acid-base disturbances.

Many studies have investigated the compensatory response to an acidosis in the context of H^+ excretion; general models for acidosis compensation in marine fishes focus on apical H^+ excretory mechanisms within the gill ionocytes (Claiborne et al. 1999; J. B. Claiborne et al. 2002; Ivanis et al. 2008; Hu et al. 2013; Edwards et al. 2005; Edwards et al. 2001). However, net transepithelial HCO_3^- uptake to buffer against an acidosis could also be a viable route to compensation. A recent study has shown that the gulf toadfish (*Opsanus beta*) is unable to defend against a respiratory acidosis when placed in HCO_3^- free water, suggesting that HCO_3^- uptake plays a crucial role in acidosis compensation (Esbaugh et al. 2012).

It has been shown that members of the slc26 protein family – slc26a3 and slc26a6 – are Cl^-/ HCO_3^- exchangers that have been implicated in ion transport in fish gills (Esbaugh et al. 2012; Bayaa et al. 2009). These proteins function as stoichiometrically opposite electrogenic transporters – slc26a3 exchanging 2 Cl^- for 1 HCO_3^- and slc26a6 exchanging 2 HCO_3^- for 1 Cl^- ion (Mount and Romero 2004). These apical proteins are mostly associated with Cl^- uptake in freshwater fishes (Bayaa et al. 2009). In seawater fishes they are presumed to be involved only in HCO_3^- excretion owing to the high environmental Cl^- that would make HCO_3^- uptake thermodynamically unfavorable. However, if slc26a3 is co-localized with the Na^+, K^+, $2Cl^-$ co-transporter (NKCC), the same electrochemical gradients that typically drive Cl^- excretion through CFTR may allow HCO_3^- uptake. This pathway would continue to excrete Cl^- while also uptaking HCO_3^- , which would meet both osmoregulatory and acid-base functions. In fact, this may be

preferable to the well-known NHE pathway, which requires Na^+ that comes at an osmoregulatory cost.

An additional slc26 member – slc26a5 – was recently identified in an in-house red drum gill/intestine transcriptome. Interestingly, this member was initially described in mammalian literature as a motor protein for inner ear sensory hair cells (Dallos and Fakler 2002). This function is independent of anion exchange capability and, in fact, mammalian slc26a5 does not show classical anion exchange function. In contrast, both chicken and zebrafish slc26a5 exhibit electrogenic anion exchange similar to slc26a6 when expressed in oocytes (Schaechinger and Oliver 2007). Despite the finding that zebrafish slc26a5 is a functional anion exchanger, no studies have examined a potential role for slc26a5 in epithelial ion transport and acid-base regulation in non-mammalian vertebrates.

With this background, this study aimed to characterize the potentials roles of slc26a3, a5, and a6 in the compensation responses of red drum to hypercapnia induced acidosis. The initial objective was to determine the relative expression of the three genes in a variety of red drum tissues, with specific emphasis on the relative expression in the gills. We then sought to assess the short-term and long-term physiological plasticity in response to environmentally relevant and physiologically extreme respiratory acidoses. The final objective was to determine if compensation from a respiratory acidosis, as measured through net H^+ excretion, was reduced in the presence of the known anion exchange inhibitor DIDS.

METHODS

Animal Handling

Sub-adult red drum were collected from Texas Parks and Wildlife hatchery in Corpus Christi, Texas, or spawned and raised at the University of Texas Marine Science Institute Fisheries and Mariculture Laboratories, Port Aransas, Texas. Fish were housed in recirculating systems with UV treated natural seawater collected from the Port Aransas ship channel. All tanks were aerated and ammonia was controlled by recirculating system water through a biofilter. Temperature was controlled using automated in-line heater/chiller units. CO_2 and pH were kept low through consistent partial water replacement using additional flow-through lines. All fish were held on a 14 h: 10 h light dark cycle. Fish were fed daily with commercially available Aquamax pelleted dry food and fish were acclimated to control conditions in the facility for at least two weeks prior to experimentation. All experiments were conducted in accordance with protocols approved the University of Texas at Austin Institutional Animal Care and Use Committee.

CO_2 Exposure

Sub adult red drum were held in 300 L recirculating tanks supplied with filtered, UV treated Port Aransas ship channel water (pH = 8.15) for at least two weeks prior to CO_2 exposure. Fish were then transferred into a 300 L exposure tank or a 300 L control tank. Food was withheld for at least 24 hours prior to sampling. Initial experiments were performed at control, 6,000 µatm, and 30,000 µatm nominal CO_2 for 4h and 24h (n= 8/ treatment, mean body weight ± S.E.M = 39.5± 5.8g). Gill samples exposed to 1,000 µatm

nominal CO_2 for 4h, 24h, 72h, and 14d with concurrent controls were obtained from a previous data set (Esbaugh et al. In Review). Additionally, 1h exposures were run at 1,000 μatm and 6,000 μatm nominal CO_2 with concurrent controls (n=8/ treatment, mean body weight ± S.E.M = 32.7± 1.5g). Each level of hypercapnia was maintained by aerating tanks with room air mixed with CO_2, control tanks were aerated with ambient room air. pCO_2 exposure levels were verified by CO_2 Calc software (Robbins et al., 2010) using pH and titratable alkalinity measurements. Immediately following exposure, specimens were euthanized with an overdose of Tricane methanesulfonate (MS 222) followed by spinal cord transection. Gill tissue samples were collected from each specimen, placed in RNALater, and subsequently stored at -80°C until processing.

Molecular Methods

Real time PCR primers were developed for two slc26a3 isoforms (slc26a3a, b), slc26a5, and slc26a6. Full length sequences for sequences were identified in an in-house gill/intestine transcriptome using Blaststation software. The identified sequences were then verified against the NCBI database using a standard Blast search. Primer pairs were identified using Primer3Plus software package (Untergasser et al., 2007). All primers and GenBank accession numbers for related sequences can be found in Table 1.

Gill lamellae stored in RNALater were washed twice in 500 μL PBS before homogenization. Total RNA isolation was performed using TriReagent according to the manufacturer's protocols. Concentration and purity of total RNA was measured using a NanoDrop ND-1000 spectrophotometer (Thermo Scientific). Total RNA was treated for

potential DNA contamination by incubating with DNase 1 (Thermo Scientific), according to manufacturer protocols. cDNA synthesis was performed on 1 µg of total RNA using RevertAidM-Mulv reverse transcriptase (Thermo Scientific), according to manufacturer protocols. For all cDNA synthesis runs, a No-RT control reaction was performed to ensure that DNase treatment removed genomic DNA contamination.. Samples were then diluted in 180 µL nuclease free water and stored at -20°C until qPCR analysis.

qPCR analysis was performed using the Maxima SYBR Green kit (Thermo Scientific). Reactions were prepared according to manufacturer protocols with the exception that a 12.5 µl total reaction volume was used. All reactions were processed using an MX3000P qPCR machine (Stratagene) with accompanying software. A serial dilution of cDNA was used to generate standard curves to determine reaction efficiency for all primer pairs. PCR efficiencies ranged from 79 to 116% with an $R^2 \geq 0.83$. For all genes, negative and no reverse-transcriptase control reactions were performed. The CT values for each sample were used to assess relative abundance of each gene in relation to the control gene elongation factor 1α (EF1-α) using the delta-delta CT method (Pfaffl 2004).

Whole Animal Acid Flux Methods

Sub-adult red drum (n=6/ treatment, mean body weight ± S.E.M = 11.6± 0.9g) were starved for 24 hours prior to and throughout the experiment. Fish were placed in individual chambers (approximately 365 mL) affixed with flow-through control seawater (salinity 32, temperature 22°C, pH 8.12) and aeration. All individuals underwent an 8 hour acclimation period prior to experimentation. After the acclimation period, the water source was

removed and individuals underwent a 16 hour control period in which basal acid flux was measured followed by a one hour flush period prior to initiating hypercapnia exposures.

Hypercapnia and DIDS exposures were initiated by removing the water source and switching aeration from ambient room air to room air mixed with 30,000 µatm nominal CO_2. Experimental chambers were inoculated with 2mM DIDS in 0.1% DMSO and control chambers were inoculated with 0.1% DMSO (Grosell, Genz, et al. 2009). For all flux periods, water samples were taken at the beginning and end of the flux period for determination of titratable alkalinity and ammonia. The exact time of each sampling point was noted and pH was measured at the onset of each flux period to verify CO_2 treatment levels. pH, temperature, titratable alkalinity and salinity measurements were also taken from the flush reservoir. At the conclusion of control and hypercapnia flux periods the individual chambers with water were weighed and the weight of the fish and empty chamber was subtracted to obtain the flux chamber volume. Known sample volume was added to the calculated flux chamber volume where appropriate.

Immediately following water sample collection, each 25 mL flux period water sample was aerated with pure N_2 gas for 15 minutes to remove any contribution of respiratory CO_2 from the sample. Samples collected to verify CO_2 treatment levels did not undergo N_2 aeration. 10 mL of each sample was then titrated at room temperature with 0.1 N HCl using an Apollo SciTech AS-ALK2 alkalinity titrator and accompanying software to determine titratable alkalinity. Ammonia concentrations were measured in each sample using a colorimetric analysis (Verdouw et al. 1978).

Statistical Methods

All gene expression data for CO_2 treatments were assessed by ANOVA against control groups with the exception of the 1h exposure to 6,000 μatm and 1,000 μatm CO_2 series which had concurrently run control groups for all time points and thus were assessed by Student's *t*-test. Changes in H^+ excretion during the DIDS exposure – against controls and between treatments – were analyzed using a two-way ANOVA. All statistical tests were performed with a fiducial level of significance of $P < 0.05$.

RESULTS

Gene Expression

qPCR analysis of gene expression was conducted on each of the four slc26 genes listed in Table 1. Initial analyses were performed to assess the relative abundance in gills of red drum (Figure 11). The most abundant transcript was slc26a5, which was almost 30-fold more abundant than other gene family member. Conversely, expression of slc26a3b and slc26a6 in the gill was generally low with only 28 % and 29 % of tested samples even showing detectable expression. Interestingly, when expressed slc26a3b was detectable, it was expressed at the same levels as slc26a3a. The expression of each gene was also tested against a tissue panel with expression normalized to the tissue with the greatest abundance (Figure 12). The slc26a3a, a3b and a6 genes were all expressed in the highest levels in the intestine. The slc26a6 gene was also expressed in relatively high abundance in the kidney, while slc26a3b was mostly absent from non-intestinal tissue. While Figure 12 may suggest that no other tissue showed detectable expression slc26a3a expression, this is simply due

to the 1000-fold higher levels of slc26a3a expression found in the intestine. In fact, slc26a3a expression was detected in all tissues in the panel. The slc26a5 gene was also expressed in a wide variety of tissues, with heart, red muscle and white muscle making up the second most abundant tissue sources. Due to the relatively inconsistent expression of slc26a3b and slc26a6 these genes were omitted from further plasticity analyses. No changes in slc26a3a or slc26a5 gene expression were observed in the initial 24h exposures to 1,000 μatm (Figure 13) or 6,000 μatm (Figure 14) CO_2 exposures. In contrast, the more severe 30,000 μatm CO_2 treatment (Figure 15) resulted in up-regulation of slc26a5 at 4 h and 24 h, while slc26a3a was significantly up-regulated at 24 h of exposure. A second series of experiments specifically examined whether gene expressions changes occurred in the crucial first hour post-acidosis; however, no changes in either gene were observed at 1,000 μatm or 6,000 μatm CO_2 (Figure 16). Finally, a longer term assessment was performed specifically at the ocean acidification relevant 1,000 μatm CO_2, but no changes were observed at either 72 h or 14 d post-exposure (Figure 17).

DIDS Exposure

Red drum exhibited negative H^+ excretion during the 16 h control period prior to inoculation with DIDS dissolved in DMSO or DMSO alone, indicating net HCO_3^- excretion under control conditions (Figure 18). Both red drum inoculated with DIDS and those treated with DMSO excreted significantly more H^+ when exposed to 30,000 μatm CO_2 than during the control period; however, there was not a significant difference in

excretion rate between the fish treated with DIDS and those treated with only DMSO after 6 hours of exposure to 30,000 μatm CO_2.

DISCUSSION

My results provide tentative support for previous studies (Esbaugh et al., 2012) suggesting that transepithelial HCO_3^- uptake may play a role in the compensation response of marine fishes to an acidosis. Using an in-house transcriptome generated from the gills and intestine, I was able to identify four members of the slc26 gene family. Interestingly, this included a previously undescribed second slc26a3 isoform, here designated slc26a3b. Of these four genes, only slc26a3a and slc26a5 were regularly expressed in the gills, with slc26a3b and slc26a6 only expressed in the gills in approximately 30 % of samples. The expression of slc26a3a in the gills provides support for the hypothesis that this protein is involved in transepithelial HCO_3^- uptake, although co-localization studies are required before this model is more fully supported. Not surprisingly, both slc26a3 genes were most abundant in the intestine, where slc26a3 has been previously implicated in water and ion transport as well as mucus secretion (Bayaa et al. 2009; Mount & Romero 2004). Perhaps more surprising was the lack of slc26a6 expression in the gills of red drum. In freshwater fishes this gene is crucial for Cl^- absorption (Bayaa et al. 2009; Boyle et al. 2015), and the 2 HCO_3^- per Cl^- stoichiometry would make it an ideal candidate for HCO_3^- pathways that would be required in the event of a systemic alkalosis. It is noteworthy that slc26a6 is expressed in the intestine and kidneys. Much like slc26a3, the role for slc26a6 in the

intestines is largely related to water absorption, while in the kidney slc26a6 is crucial for sulfate transport (Boyle et al. 2015; Mount & Romero 2004).

Further evidence that slc26a3 may be involved in HCO_3^- uptake was obtained from the gene expression responses to a respiratory acidosis. While no change in slc26a3a expression was observed at any time point during the 1,000 μatm or 6,000 μatm CO_2 exposures, significant up-regulation did occur after 24 h of exposure to 30,000 μatm CO_2. The most parsimonious explanation for this response is that slc26a3 is involved in a physiological pathway related to net acid excretion; however, it is important to note that further experimentation is required to more fully demonstrate this pathway. These responses likely didn't occur at the lower CO_2 levels simply because there was sufficient baseline acid-base machinery to compensate for these disturbances. This is supported by previous data (Chapter 2), which have shown that these acid-base disturbances are fully compensated by 2 h post-exposure.

Another surprising finding of this study was that slc26a5 was almost 30-fold more abundant in the gills than any other member of the slc26 gene family. Furthermore, slc26a5 was also the most widely expressed member of the gene family with detectable expression in all tissues that were tested, but particularly abundant expression in the gills and three types of muscle. It had been thought this protein was only found in hair cells (Mount and Romero 2004; Tan et al. 2011); however, these results clearly are cause for reassessment of the role of this protein in epithelial transport processes. Similar to slc26a3, slc26a5 also showed significant up-regulation in the 30,000 μatm exposure, with no change in expression at lower CO_2 levels. Again, this suggests some sort of role in net acid excretion;

however, in this case the exact pathway is less clear. For example, the stoichiometry of slc26a5 is better suited for HCO_3^- excretion; however, that applies only if slc26a5 is an apical protein. If slc26a5 is basolateral then a role in HCO_3^- transport into the plasma becomes possible. Preliminary immunofluorescence performed in the Esbaugh lab (data not shown) appears to localize slc26a5 to accessory cells in the gill. These cells are found next to seawater ionocytes; however, it is unclear if the protein is basolateral or apical due to the lack of appropriate membrane marker for these cells. Importantly, these cells are also known as glycogen rich cells, which provide glucose and other metabolites to the adjacent mitochondrial rich ionocytes (Tseng et al. 2007). It seems likely that during an acidosis ionocytes require more energy, and subsequently more metabolic substrate. It is possible that the metabolic production of glucose from glycogen, or alternatively the regeneration of glycogen during recovery, is associated with an intracellular acid-base disequilibrium necessitating HCO_3^- transport.

During the acid flux experiment, DIDS – a known slc26 inhibitor (Boyle et al. 2015; Mount and Romero 2004) had no effect on net H^+ excretion during the initial 6 h of exposure to 30,000 μatm CO_2. If slc26a3 functions in HCO_3^- uptake then I would have predicted a reduction in net excretion in the presence of DIDS. The lack of impact of DIDS on H^+ excretion suggests that HCO_3^- uptake pathways are not involved in compensation to a respiratory acidosis. However, there are a number of factors that make this conclusion doubtful. First, while slc26a3 is inhibited by DIDS, its sensitivity has been debated. For example, 2 mM DIDS only inhibited slc26a3 function in oocytes by 66% (Chernova et al. 2003). Importantly, the use of seawater may further reduce the effectiveness of a 2 mM

dose. Secondly, it is well-known that other H^+ excretion pathways are present in the gills of marine fishes (see Chapter 2)(Claiborne et al. 1999; J. B. Claiborne et al. 2002; Edwards et al. 2005). Importantly, the model I proposed for slc26a3 function is dependent on Cl^- excretion. The need for Cl^- excretion stems from the gastrointestinal uptake of ions that is integral for the absorption of imbibed seawater (Grosell 2006; Loretz 1995; Marshall and Grosell 2005); however, Cl^- availability may become limiting during extreme acid disturbances such as the 30,000 μatm exposure used here. Under these scenarios, the NHE pathway is more likely to dominate as it utilizes the high concentrations of Na^+ in seawater to drive transport. It may be possible that an anion exchange pathway is optimized to defend low level disturbances, while the NHE pathway defends severe disturbances.

Overall conclusions from the gene expression data appear to be contradictory to those of the pharmacology data. Gene expression data indicates that slc26 genes may play a role in compensation to an acidosis induced by high level hypercapnia via transepithelial HCO_3^- uptake. However, pharmacology data indicates that inhibition of HCO_3^- uptake does not have an effect on net acid excretion. One possible explanation for this dichotomy is that the slc26 genes expressed in the gills are not the primary route of compensation. These data suggest that the dominant pathway for compensation is not via HCO_3^- uptake, but through H^+ excretion across the gills. If H^+ excretion is the primary compensation pathway then high levels of H^+ excreted across the gills may have overwhelmed the effects of DIDS inhibition on HCO_3^- pathways and masked the effects of DIDS on acidosis compensation. While it is obvious that the slc26 genes present in the gills of red drum exhibit phenotypic plasticity under extreme hypercapnia exposures, their roles within the

acid-base regulation pathways are still unclear. Further work on this topic is needed to establish how these genes function within ionocytes of red drum gills.

Tables and Figures

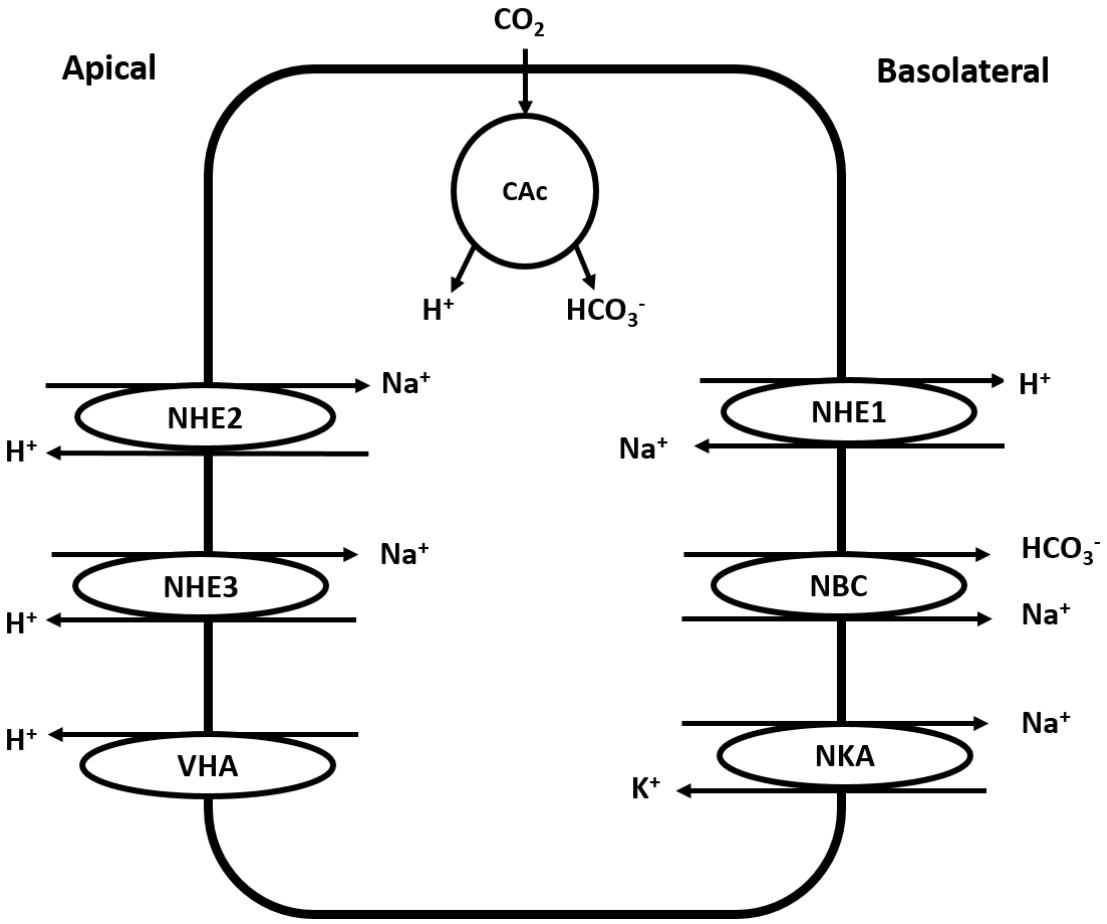

Figure 1: Generalized schematic depicting the acid-base regulatory pathways in acid secreting gill ionocytes.

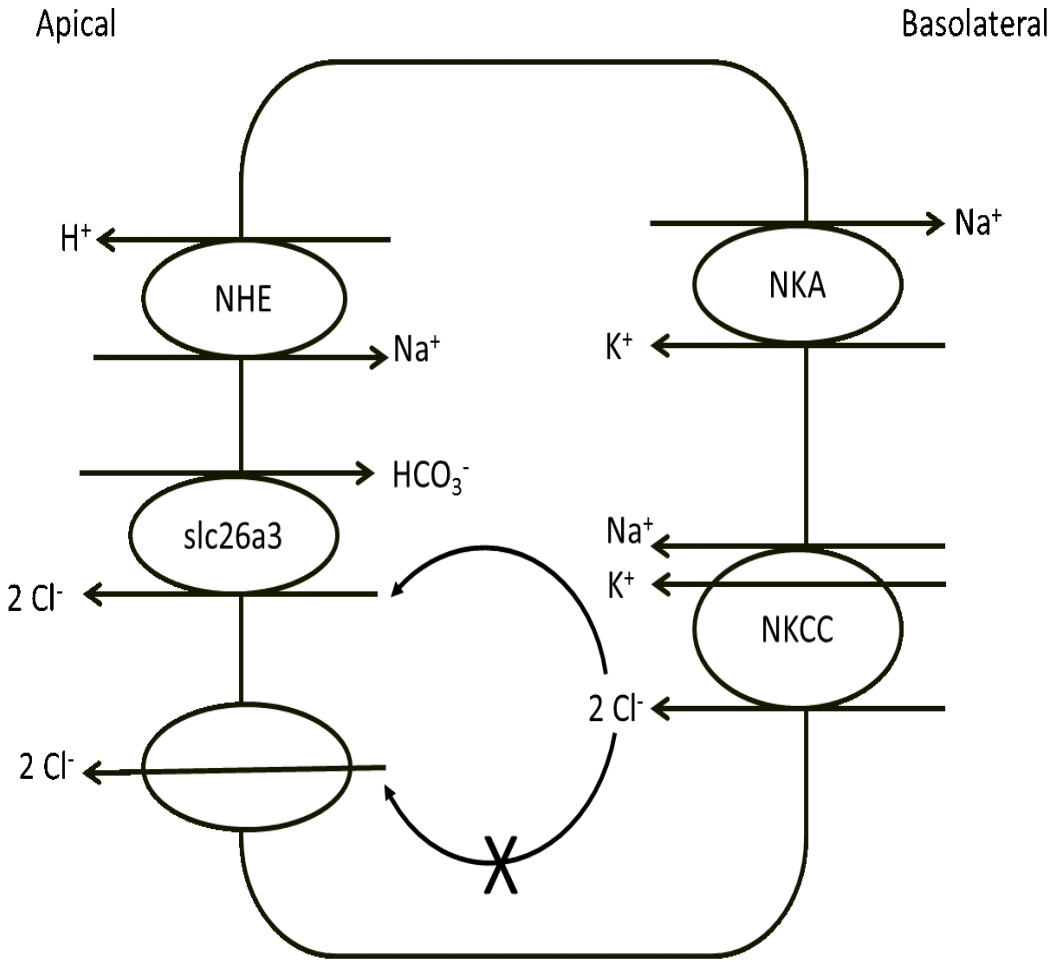

Figure 2: Proposed thermodynamically favorable slc26a3 pathway for HCO_3^- uptake and Cl^- excretion.

Table 1: List of primers used for real time PCR. All sequences are 5' to 3' and reverse primers are reverse compliments of the genetic sequence.

Gene	Accession #	Orientation	Sequence
ef1a[1]	KJ958539	F	GTTGCTGGATGTCCTGCACG
		R	GTCCGTGACATGAGGCAGACTG
NHE-1		F	AATGAGCTGCTGCACATCCTCG
		R	CAGACCACTCCGAGGACAGC
NHE-2[1]	KJ958540	F	CGGTTAAGCCTGATGGCCCTC
		R	TTGCAAACGAAGCCAGCAGC
NHE-3[1]	KJ958541	F	CAAGGTGCAGACCTTCACGCTG
		R	ACGAGGATGGCTCCCATGTT
CAc[1]	KM387716.1	F	TGACATTCGCAGACGACTCCGA
		R	AGCAGGATACTTGGTCCCTTCCA
NBC	KM387714.1	F	TCTTCATCTACGACGCTTTCAA
		R	TCATATTGAGTGACGAGGTTGG
VHA		F	CCTACCATTGAGCGTATCATCA
		R	CGTAGGAGCTCATGTCAGTCAG

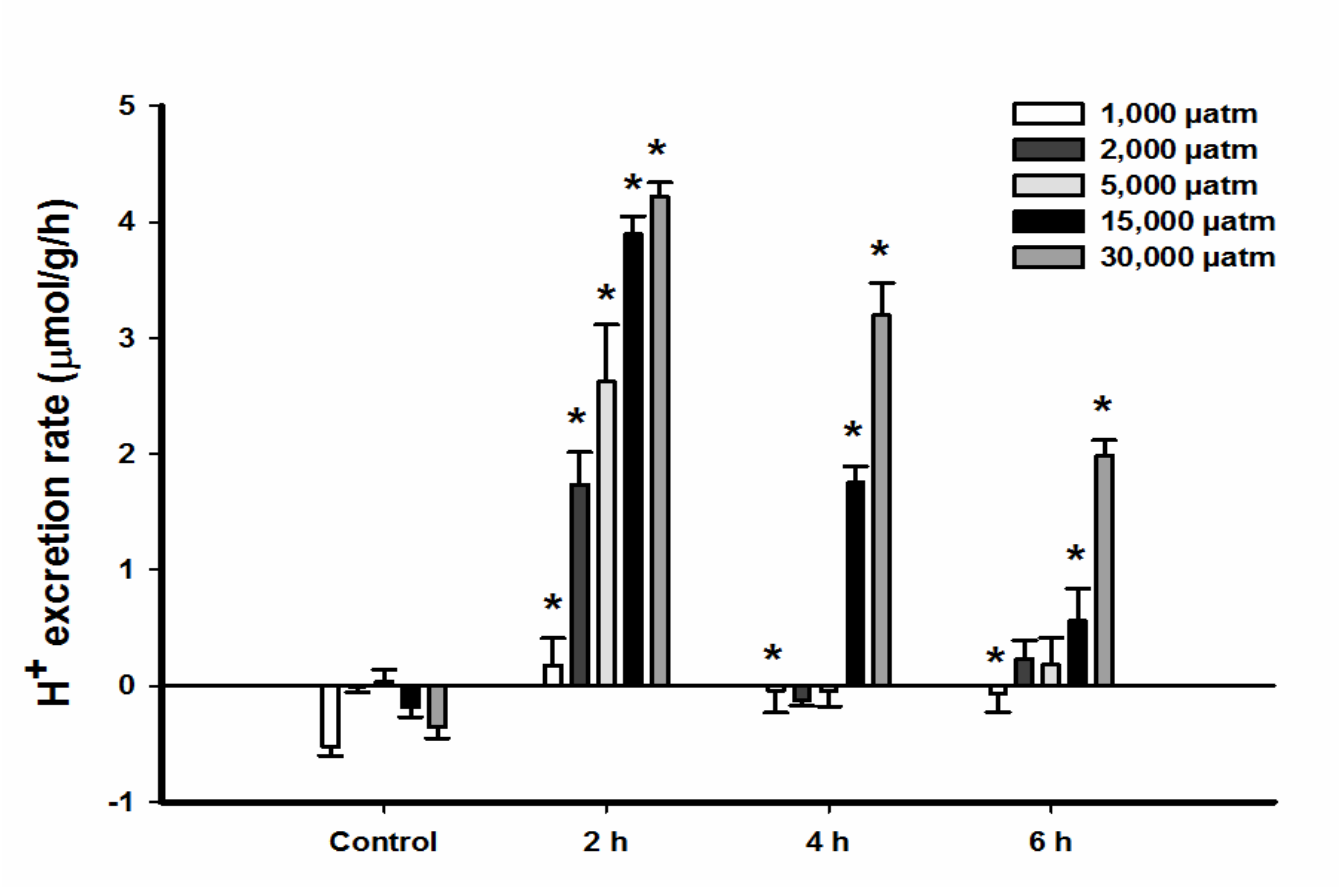

Figure 3: Net H^+ excretion rates of red drum during control period and during 6 h post exposure to 1,000, 2,000, 5,000, 15,000 or 30,000 µatm CO_2. Significant differences from controls denoted by an asterisk (ANOVA, $P<0.05$). All values are mean ± S.E.M. 1,000 µatm *N = 6*, 2,000 µatm *N = 5*, 5,000 µatm *N =12*, 15,000 µatm *N = 6*, 30,000 µatm *N=6*.

Table 2: Water quality variables throughout acid flux experiments at varying levels of CO_2.

Experiment	Dose	Temperature (^{o}c)	Salinity	pH	Alkalinity (mmol)	Pco_2
Dose response	1,000 µatm CO_2	22 ± 1	30 ± 1	7.81 ± 0.02	2195 ± 46	1074 ± 27
	2,000 µatm CO_2	23 ± 1	33 ± 1	7.59 ± 0.03	2134 ± 22	1756 ± 131
	5,000 µatm CO_2	23 ± 1	34 ± 1	7.15 ± 0.07	2160 ± 19	5373 ± 832
	15,000 µatm CO_2	23	32	6.69 ± 0.01	2318 ± 9	16281 ± 549
	30,000 µatm CO_2	24	32	6.33 ± 0.02	2327 ± 3	38317 ± 1466
Amiloride exposure (30,000 µatm CO_2)	Amiloride (1mm)	22	31	6.38 ± 0.07	2075 ± 10	31364 ± 4822
	DMSO (0.1%)	22	31	6.34 ± 0.06	2082 ± 13	33589 ± 4046

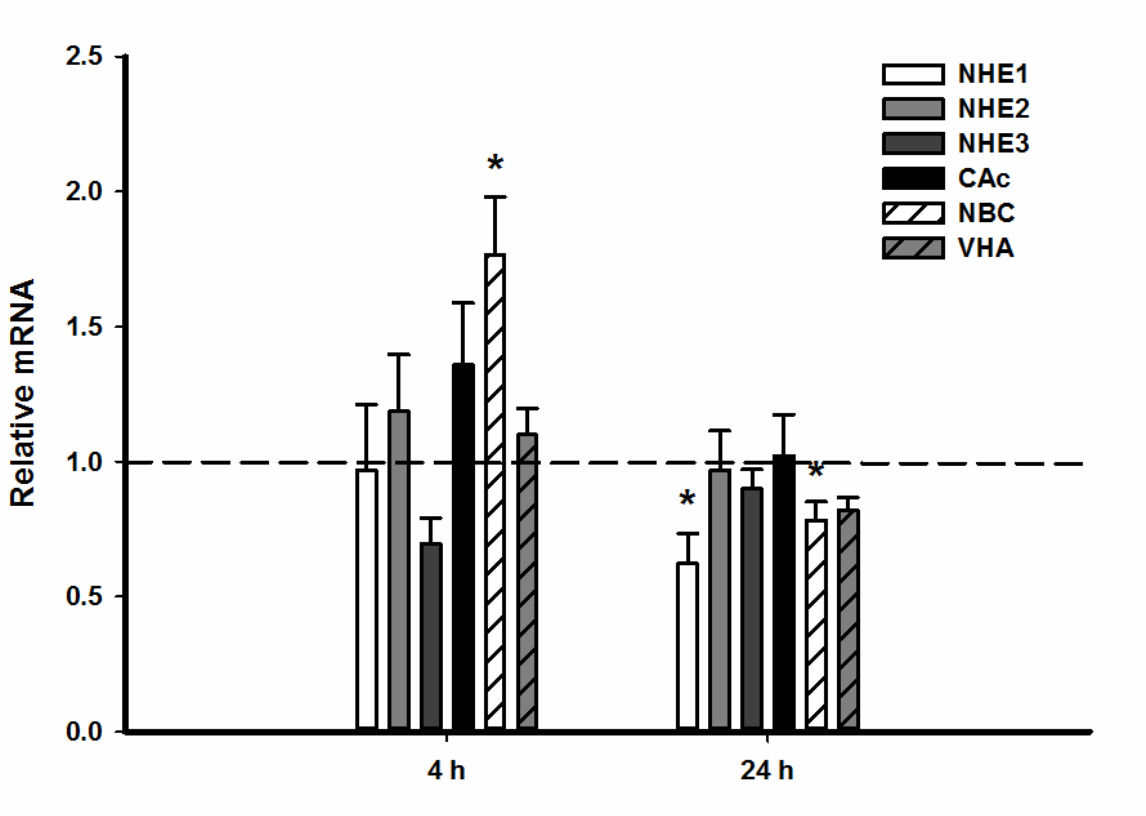

Figure 4: Gill expression of H^+ excretion pathways during initial 24 h exposure to 1,000 µatm nominal CO_2. Values set relative to control values (dashed lines at 1.0). Significant differences from controls denoted by an asterisk. All values mean ± S.E.M. *N=7-8*.

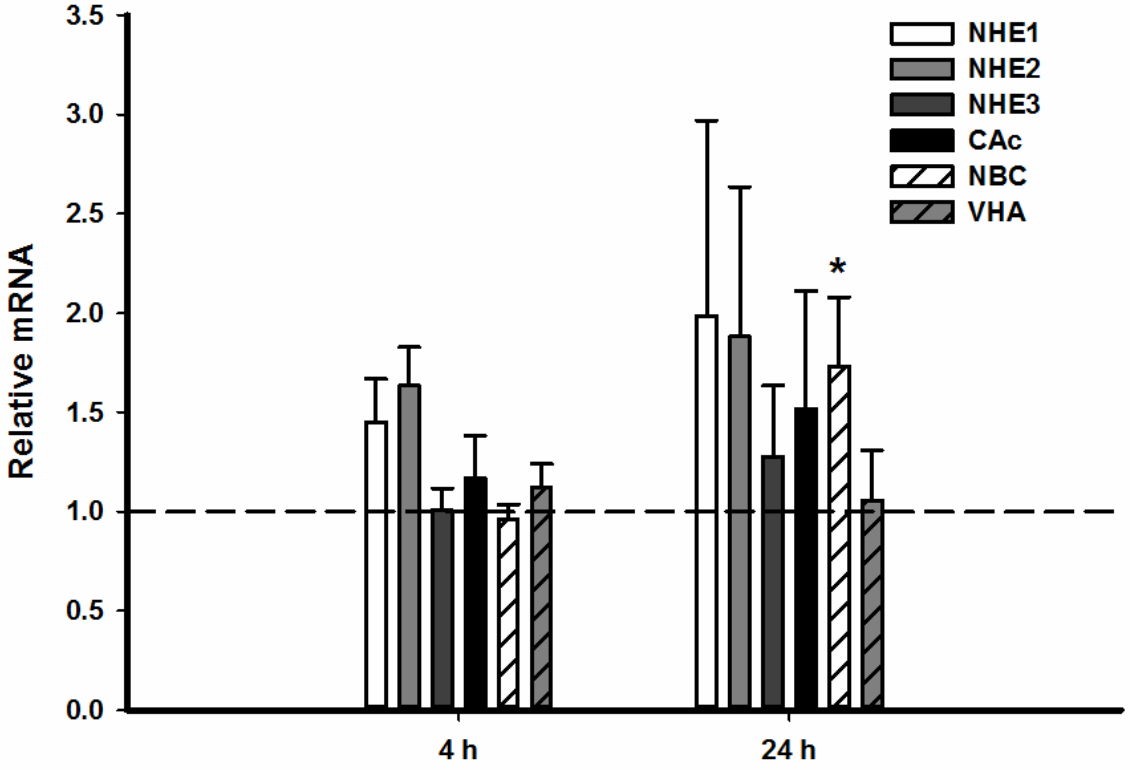

Figure 5: Gill expression of H^+ excretion pathways during initial 24 h exposure to 6,000 µatm nominal CO_2. Values set relative to control values (dashed lines at 1.0). Significant differences from controls denoted by an asterisk. All values mean ± S.E.M. *N=8*.

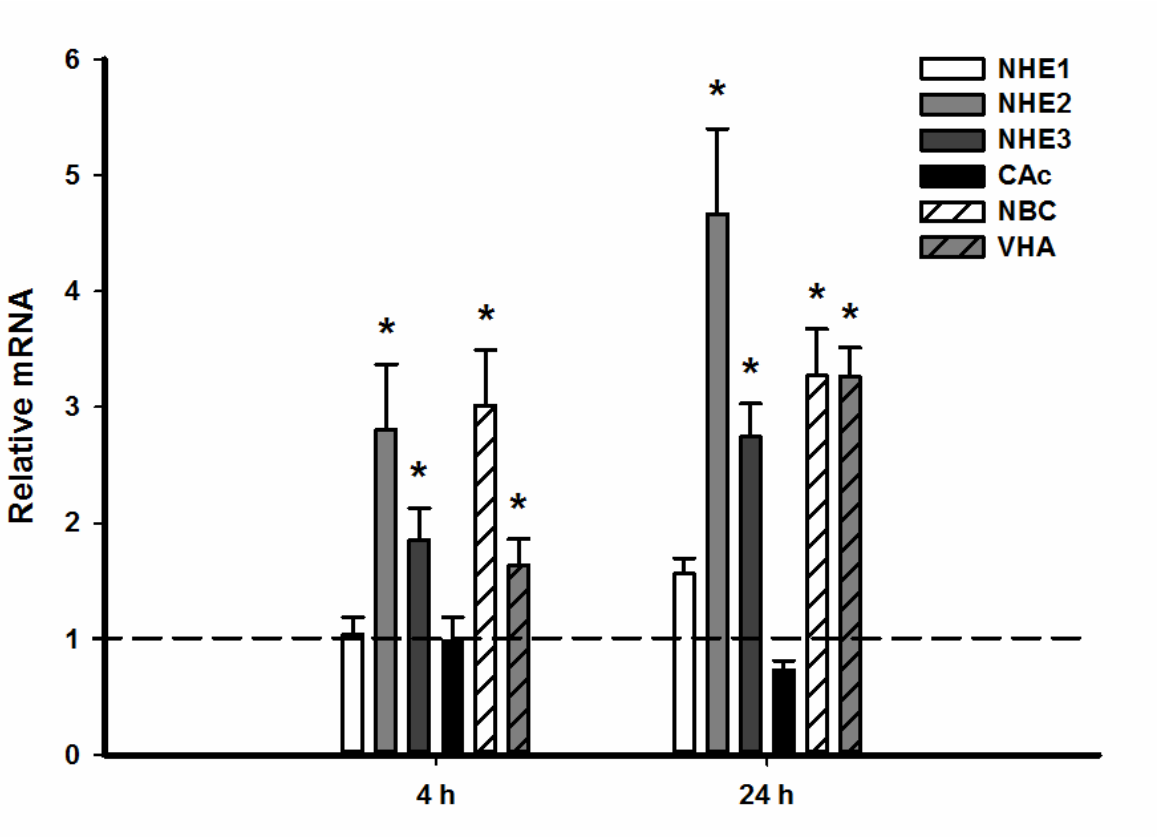

Figure 6: Gill expression of H^+ excretion pathways during initial 24 h exposure to 30,000 µatm nominal CO_2. Values set relative to control values (dashed lines at 1.0). Significant differences from controls denoted by an asterisk. All values mean ± S.E.M. *N=8*.

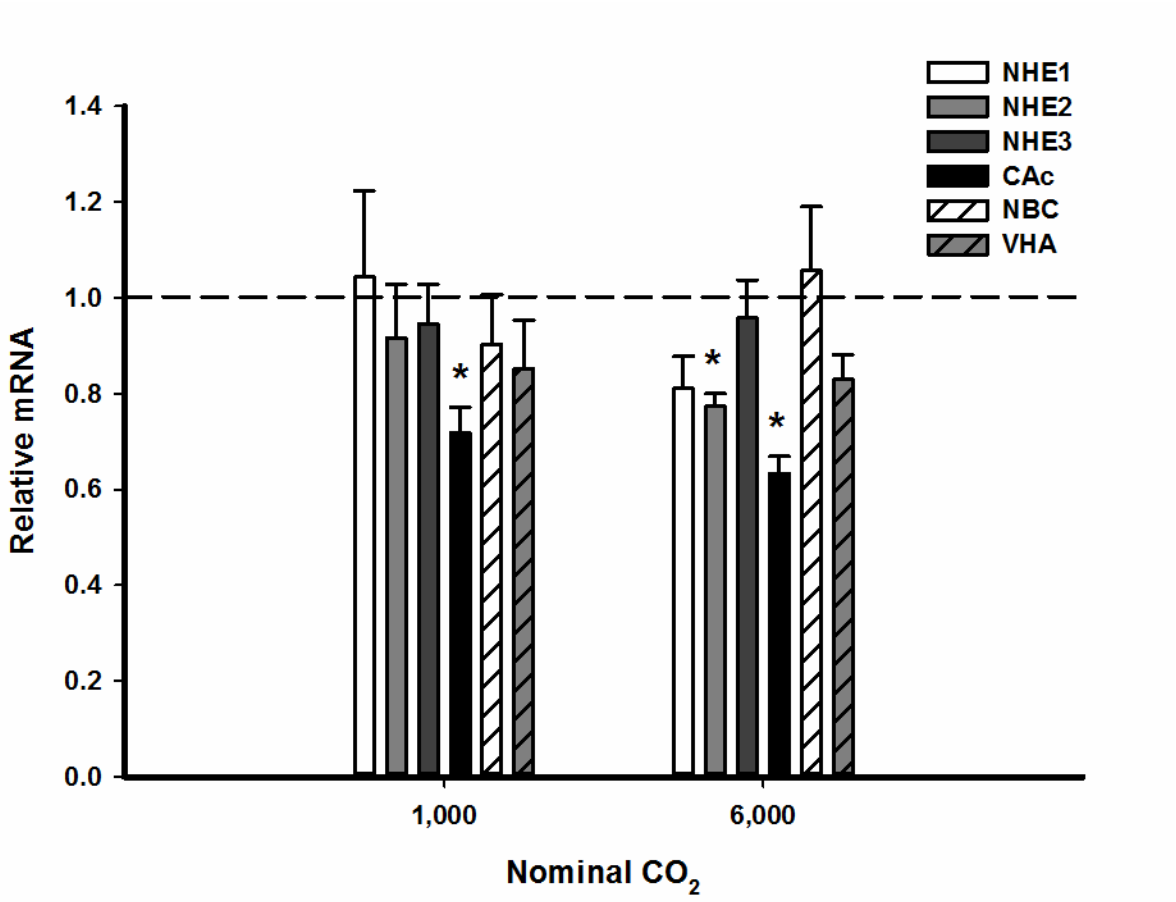

Figure 7: Gill expression of H^+ excretion pathways during 1 h exposure to 1,000 µatm and 6,000 µatm nominal CO_2. Values set relative to control values (dashed lines at 1.0). Significant differences from controls denoted by an asterisk. All values mean ± S.E.M. *N=8*.

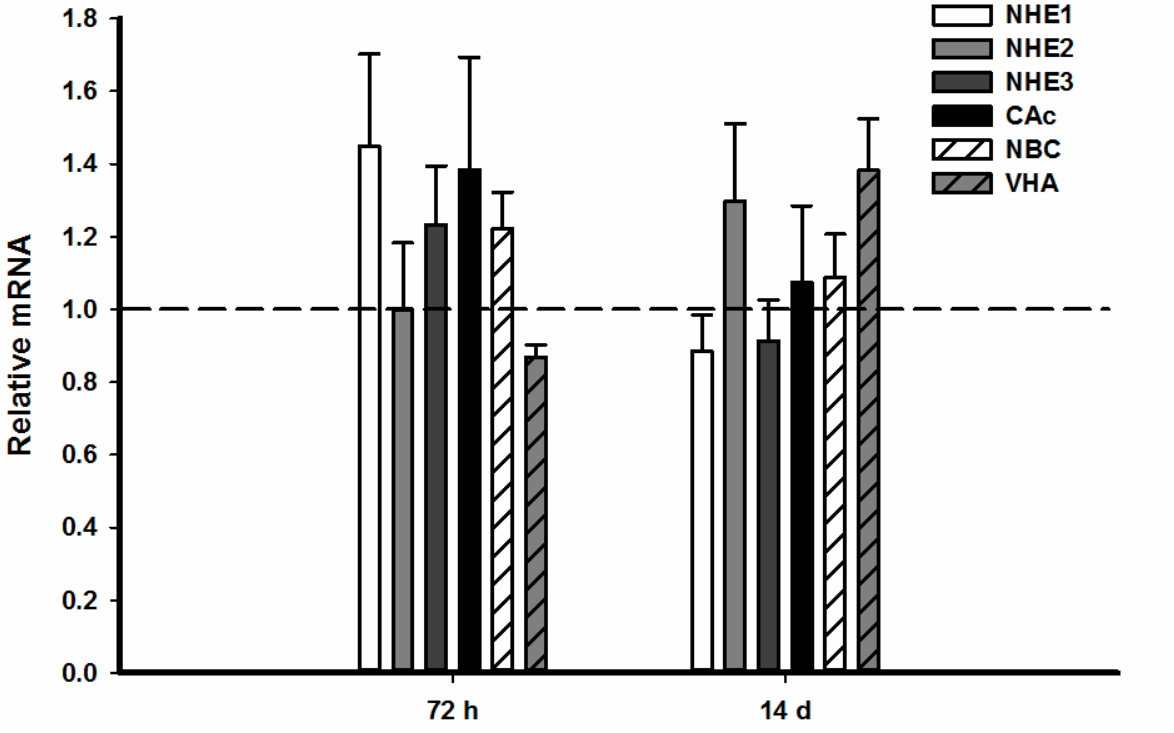

Figure 8: Gill expression of H^+ excretion pathways during prolonged exposure (72 h and 14 d) to environmentally relevant 1,000 μatm nominal CO_2. Values set relative to control values (dashed lines at 1.0). All values mean ± S.E.M. *N*=7.

Table 3: Water quality variables throughout CO_2 exposure experiment.

Dose	Temperature (°C)	Salinity	pH	Alkalinity (mmol)	pCO_2
Control	23	32	8.15 ± 0.01	2,394 ± 17	477 ± 13
1,000 µatm	23	32	7.80 ± 0.01	2,348 ± 2	1,154 ± 35
6,000 µatm	23	32	7.13 ± 0.01	2,488 ± 13	6,181 ± 77
30,000 µatm	23	32	6.44 ± 0.01	2,346 ± 1	29,159 ± 364

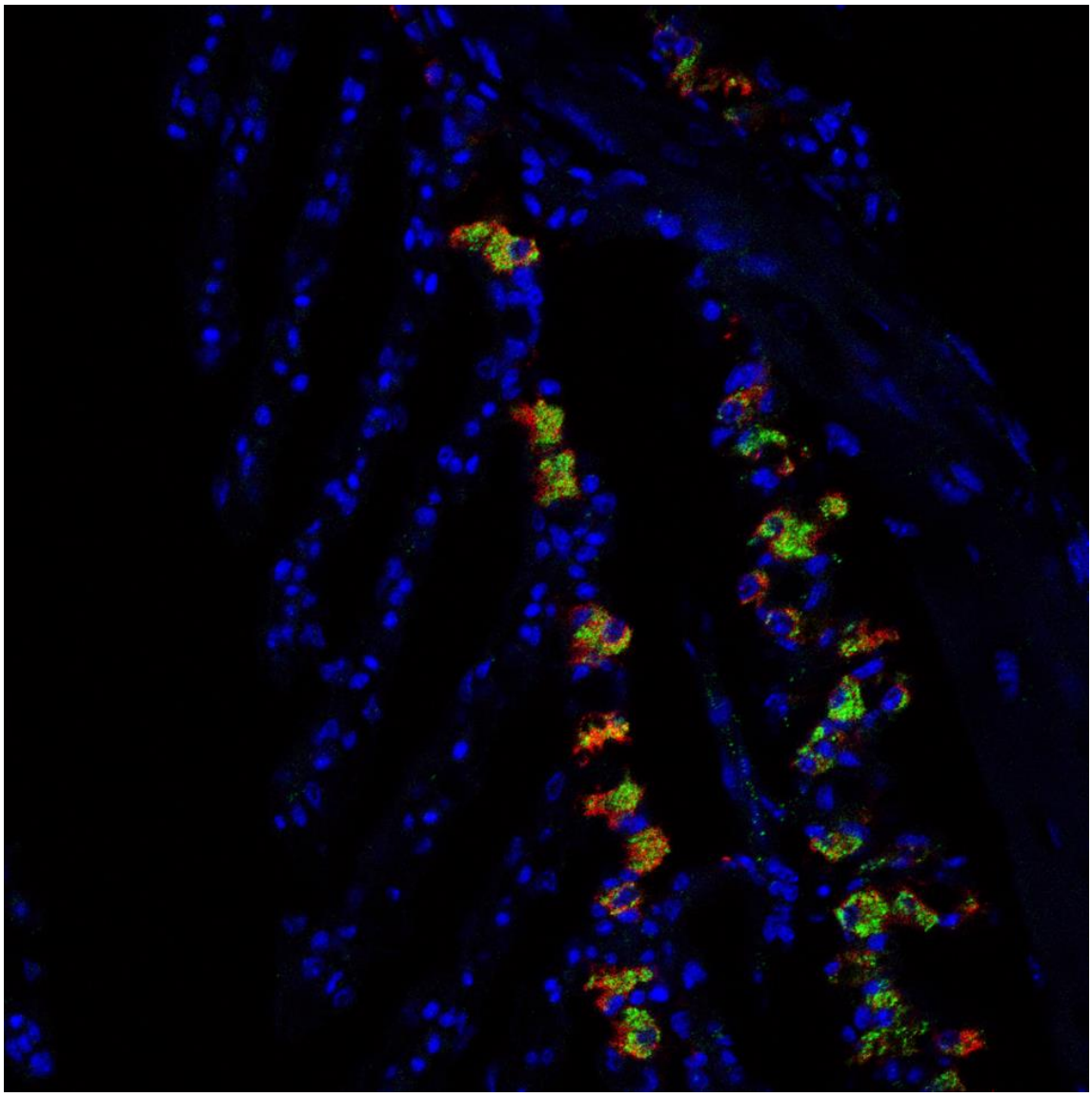

Figure 9: Dual immunolocalization of Na^+K^+ ATPase (NKA; red) and V-Type ATPase (VHA; green) within control red drum gill ionocytes. NKA is localized to basolateral membrane while VHA is diffusely distributed throughout cytoplasm.

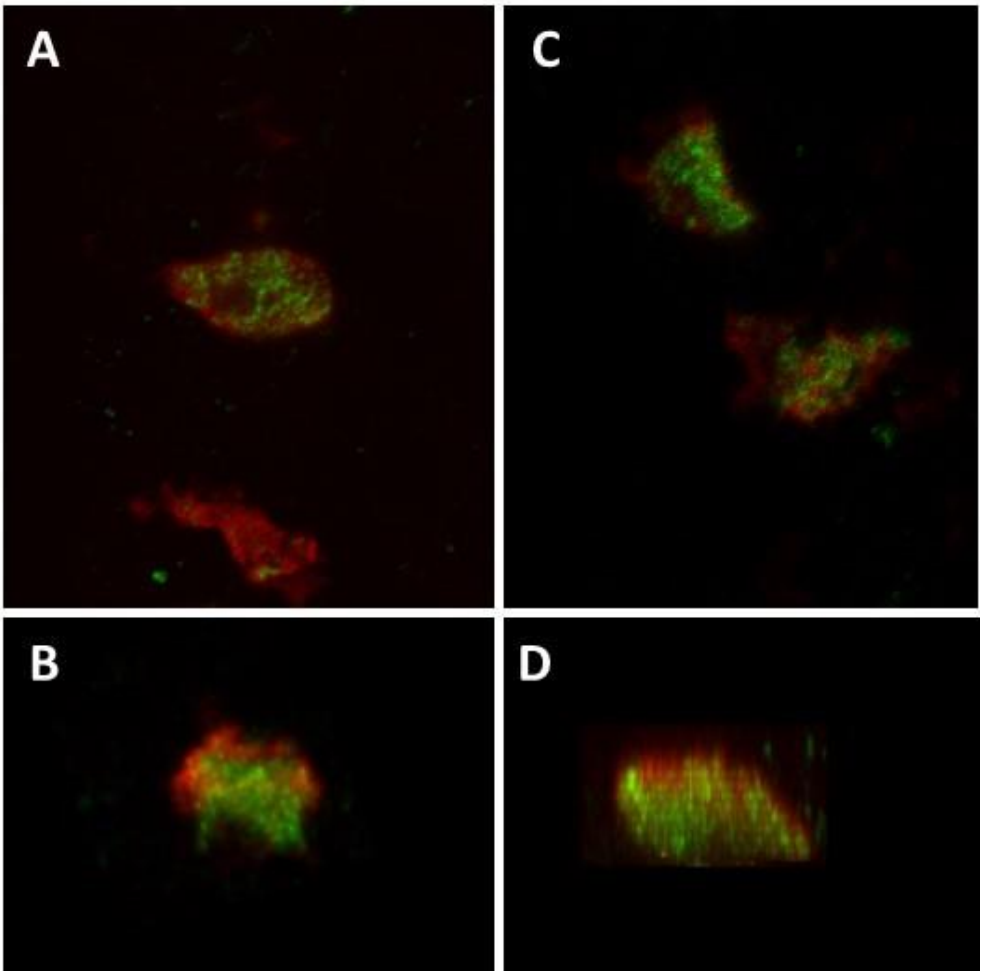

Figure 10: Dual immunolocalization of NKA (red) and VHA (green) within red drum gill ionocytes. A) Top down view of control ionocyte. B) Rotated view of a single control ionocyte with NKA clearly localized to basolateral membrane and VHA diffusely distributed throughout cytoplasm. C) Top down view of gill ionocyte exposed to 6,000 μatm CO_2. D) Rotated view of a single ionocyte exposed to 6,000 μatm CO_2 with NKA localized to basolateral membrane and VHA in cytoplasm near the apical pole.

Table 4: List of primers used for real time PCR. All sequences are 5' to 3' and reverse primers are reverse compliments of the genetic sequence.

Gene	Orientation	Sequence
ef1a [1]	F	GTTGCTGGATGTCCTGCACG
	R	GTCCGTGACATGAGGCAGACTG
slc26a3-a	F	CAACTGTTGCTTCTTTGACGAC
	R	AGTCTGGGTGTTTCTCGATGAT
slc26a3-b	F	CAAGGCACACAGGAAAATCA
	R	GGGAAGCTCTTCCATGTTCA
slc26a5	F	GGGGATTAAGATTTTCCACTCC
	R	GGTTTACTCCCGTCTTCTCCTT
slc26a6	F	TGCCAGGGATTTTGATCTTC
	R	GTTTCTTCTTTGCCGACAGG

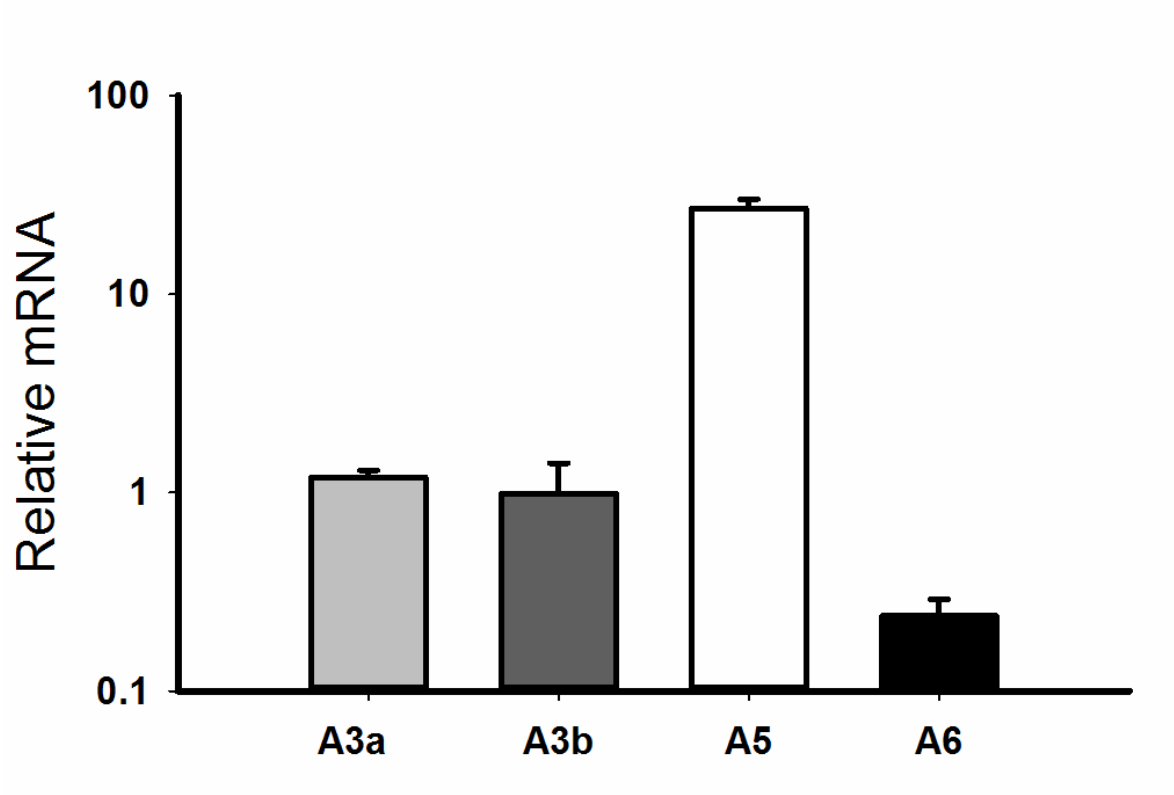

Figure 11: Baseline expression of four members of the slc26 gene family in red drum gills. Values are mean ± S.E.M relative to slc26a3a expression and normalized using ef1α.. slc26a3a *N = 64*, slc26a3b *N =19*, slc26a5 *N = 68*, slc26a6 *N = 20*.

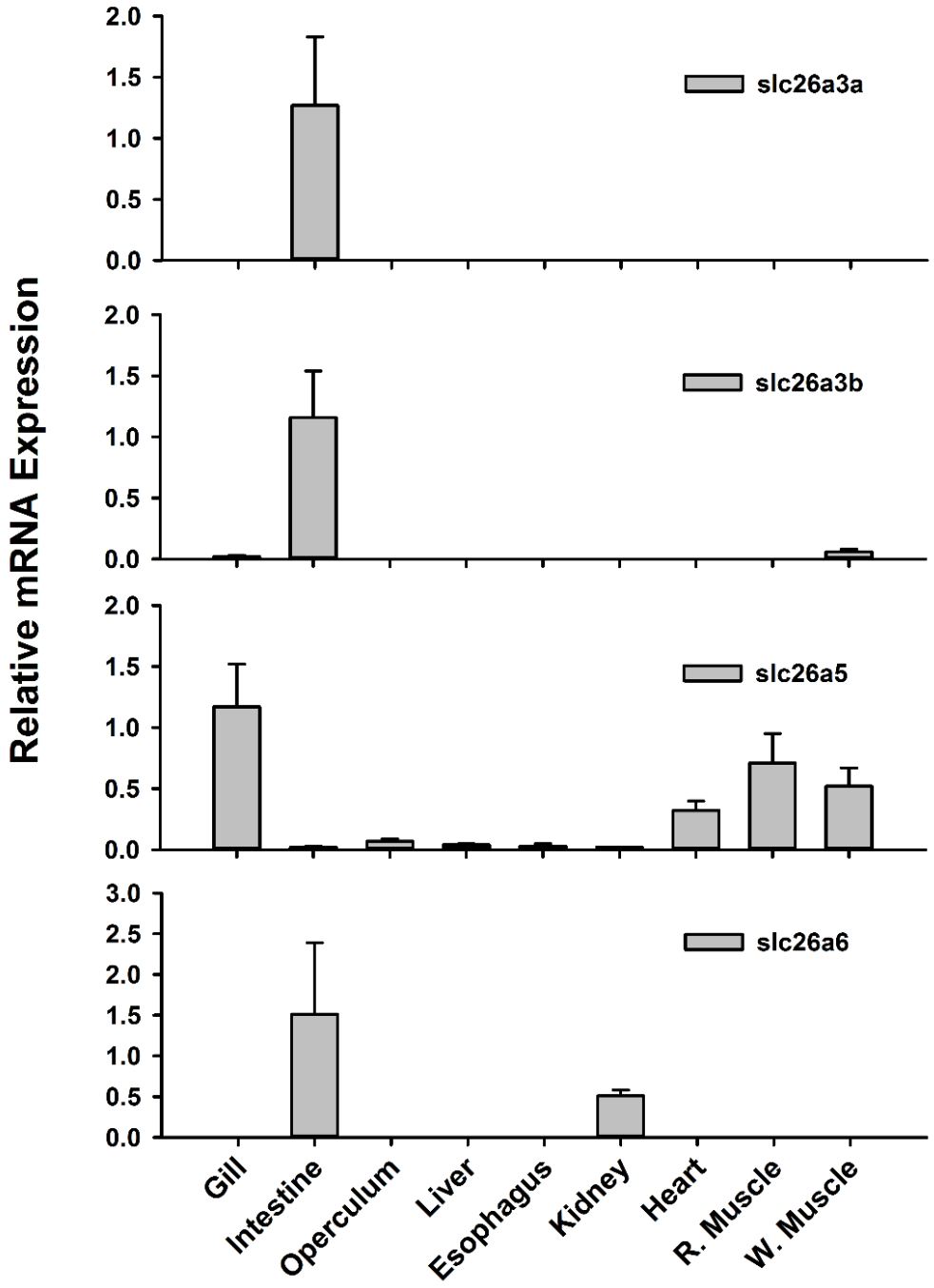

Figure 12: Tissue distribution panel of four slc26 genes identified within red drum transcriptome (slc26a3a, slc26a3b, slc26a5, slc26a6. Relative expression is calculated in relation to the tissue with highest abundance. All values mean ± S.E.M. For all tissues *N = 4*.

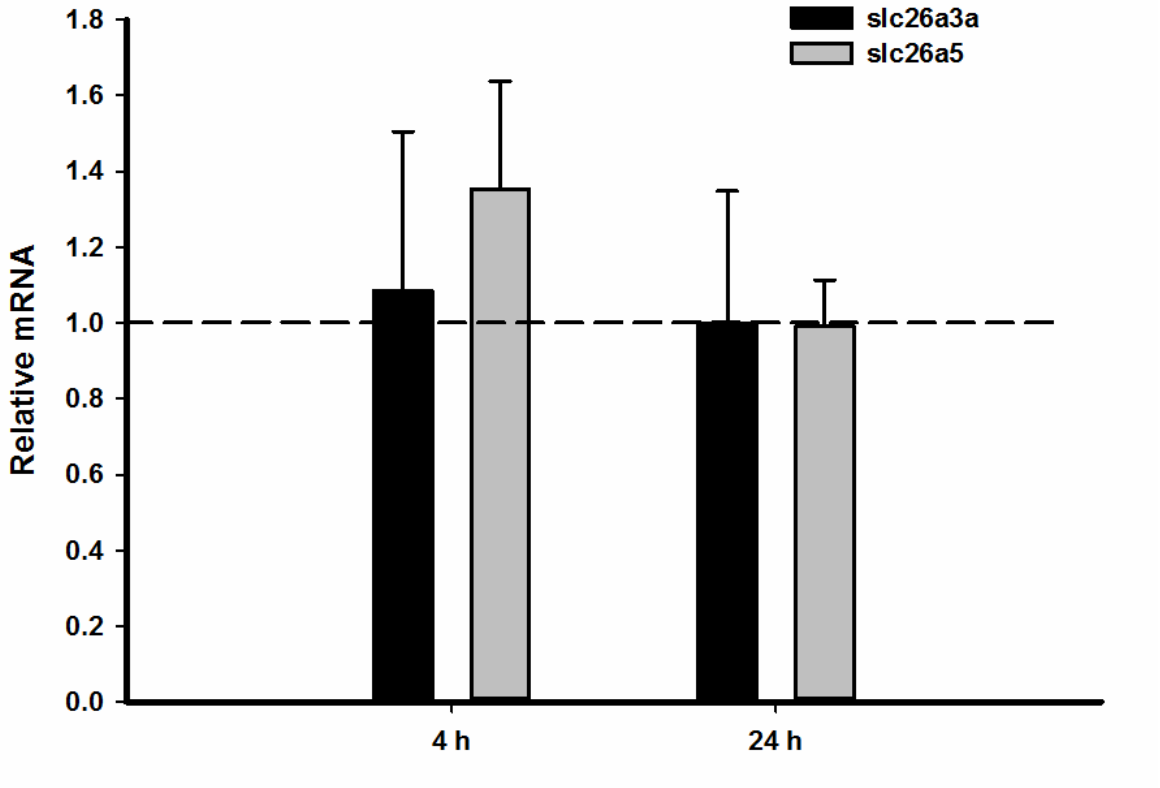

Figure 13: Gill expression of slc26a3a and slc26a5 during at 4 h and 24 h of exposure to 1,000 µatm nominal CO_2. Values set relative to control values (dashed lines at 1.0). All values mean ± S.E.M. *N=7-8*.

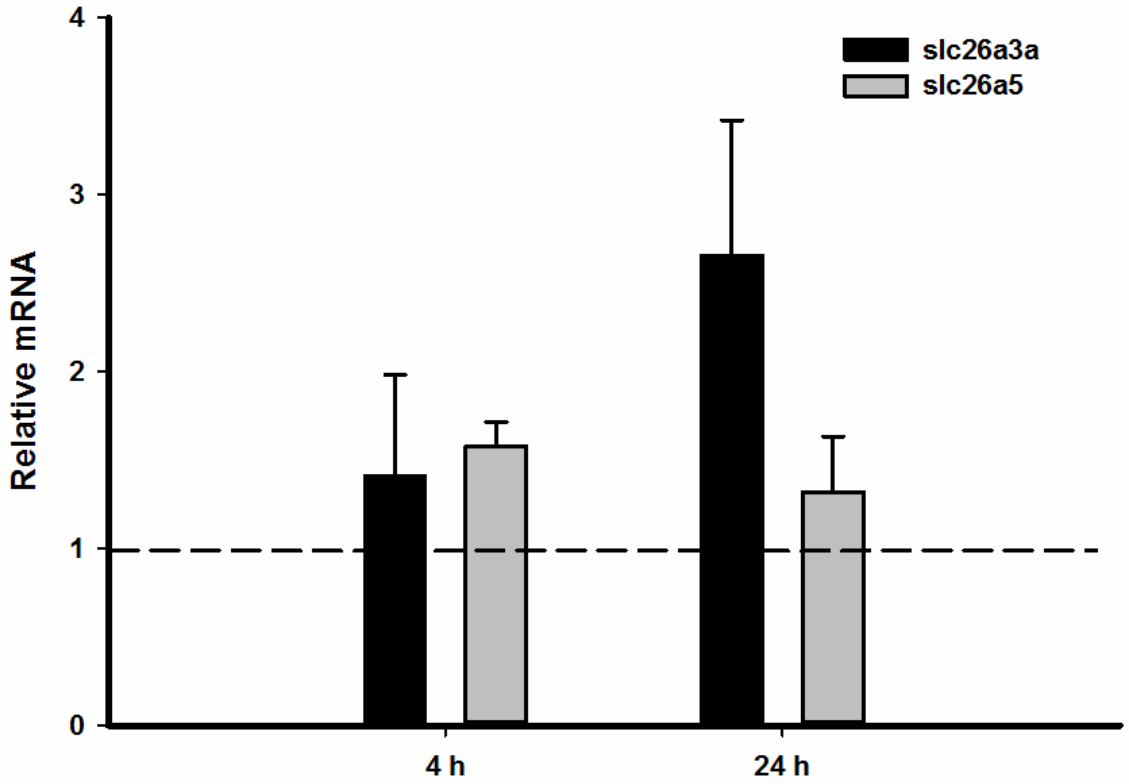

Figure 14: Gill expression of slc26a3a and slc26a5 during initial 24 h exposure to 6,000 µatm nominal CO_2. Values set relative to control values (dashed lines at 1.0). All values mean ± S.E.M. *N=7-8*.

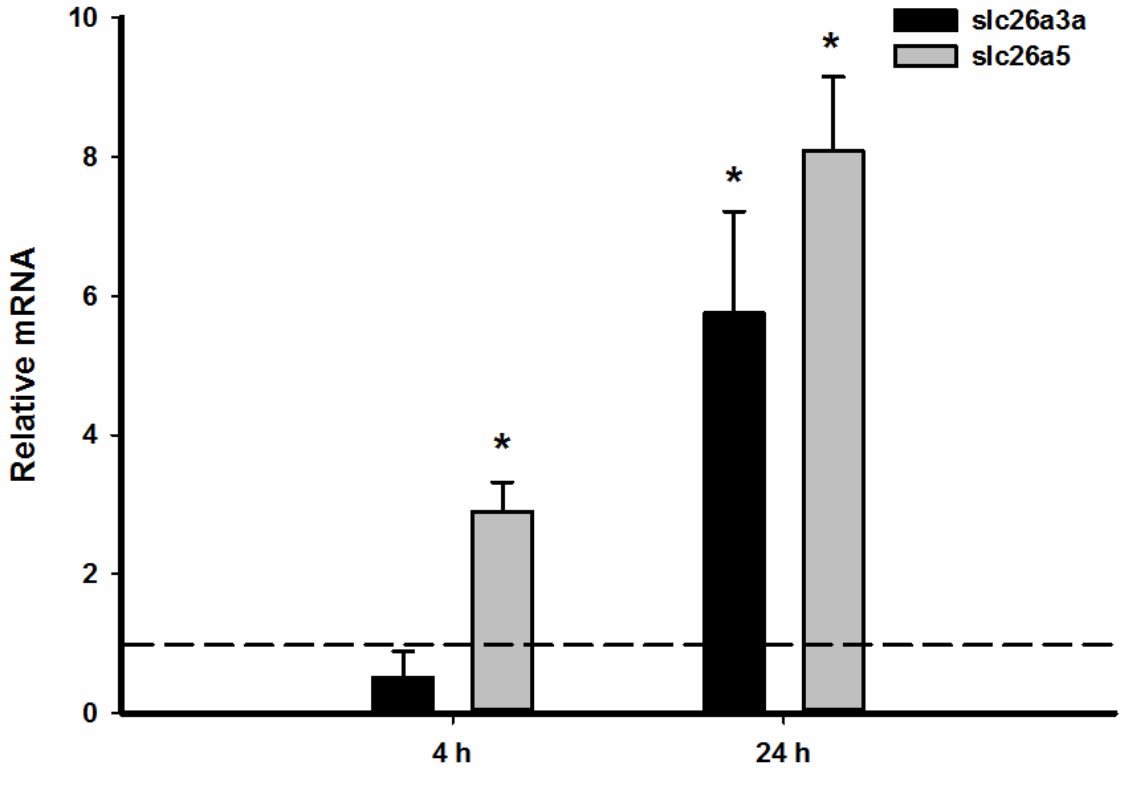

Figure 15: Gill expression of slc26a3a and slc26a5 during initial 24 h exposure to 30,000 µatm nominal CO_2. Values set relative to control values (dashed lines at 1.0). Significant differences from controls denoted by an asterisk. All values mean ± S.E.M. *N=7-8*.

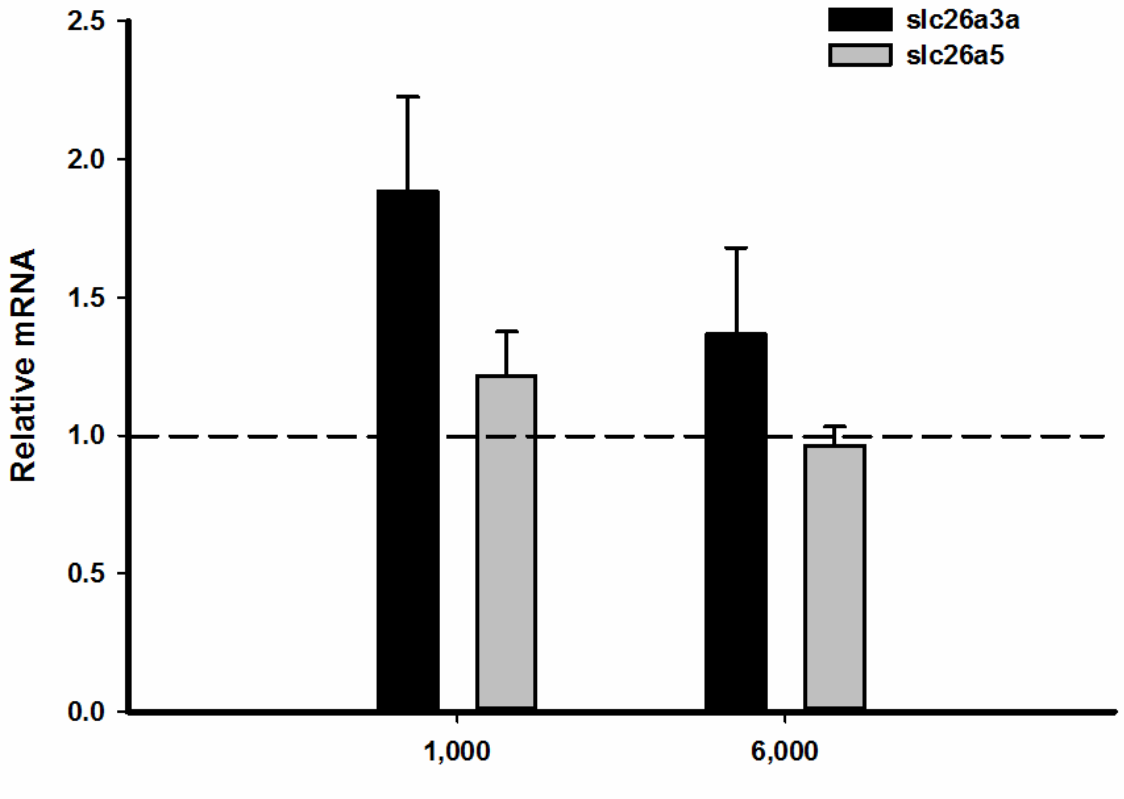

Figure 16: Gill expression of slc26a3a and slc26a5 during 1 h exposure to 1,000 µatm and 6,000 µatm nominal CO_2. Values set relative to control values (dashed lines at 1.0). All values mean ± S.E.M. *N=8*.

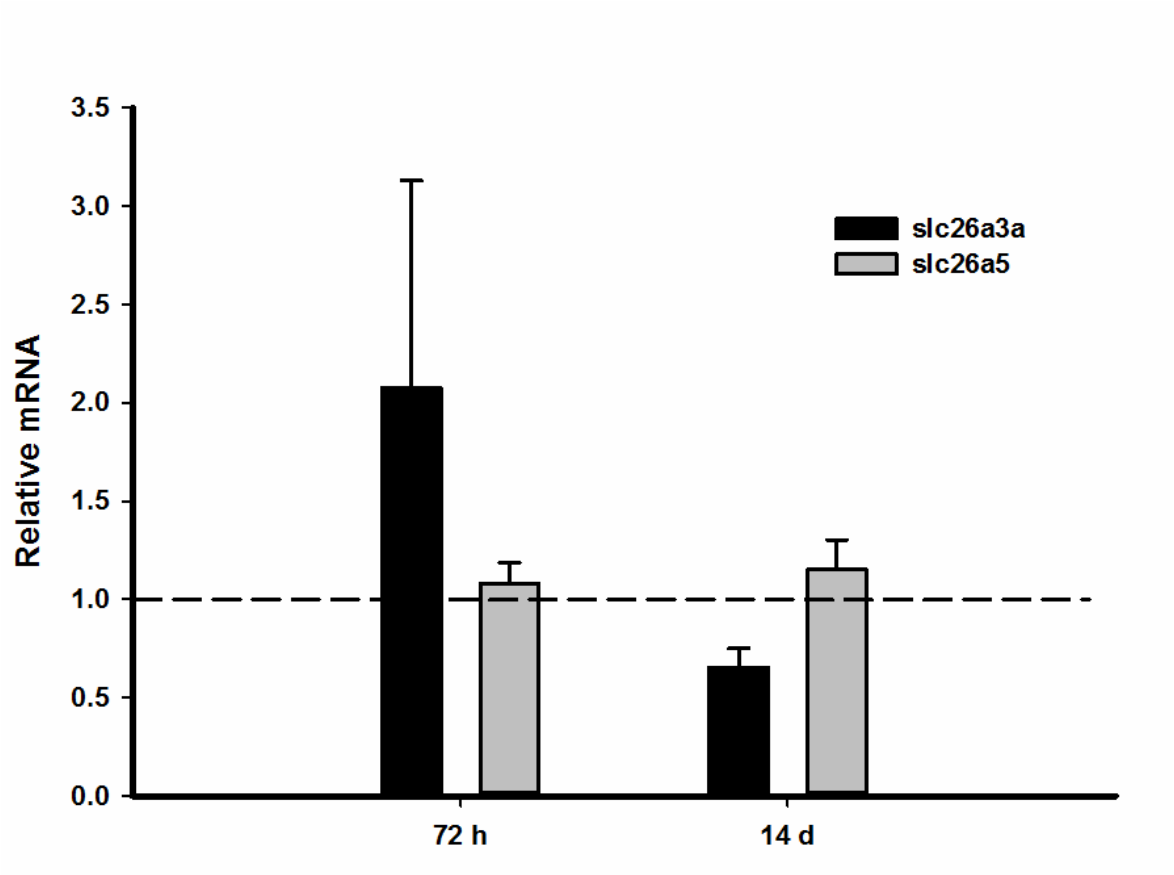

Figure 17: Gill expression of slc26a3a and slc26a5 during prolonged exposure (72 h and 14 d) to environmentally relevant 1,000 µatm nominal CO_2. Values set relative to control values (dashed lines at 1.0). All values mean ± S.E.M. *N=7*.

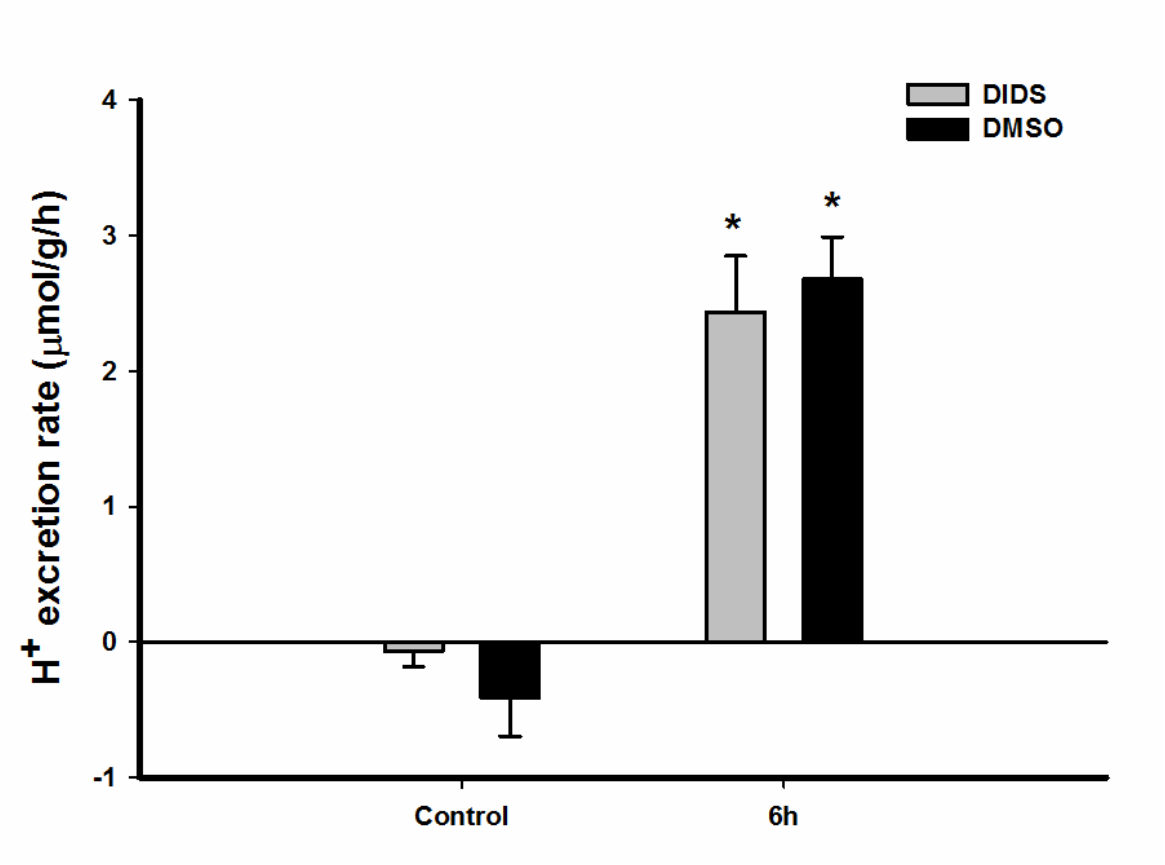

Figure 18: Net H^+ excretion rates of red drum exposed to 30,000 μatm CO_2 in the presence of either 2 mM DIDS or 0.1% DMSO. Control flux was performed in the absence of either drug or vehicle. Significant differences from controls denoted by an asterisk (ANOVA, $P<0.05$); no differences were observed between DIDS and DMSO treatments. All values are mean ± S.E.M. *N=6*.

Table 5: Water quality parameters during acid flux experiments in the presence of the anion exchange inhibitor DIDS.

Treatment	Temp (°C)	Salinity	pH	Alkalinity (mM)	pCO_2 (µatm)
DIDS (2mm)	23	32	6.33 ± 0.01	2160 ± 44	34816 ± 1473
DMSO (0.1%)	23	32	6.40 ± 0.03	2291 ± 13	31935 ± 1753

References

Bayaa, M. et al., 2009. The involvement of SLC26 anion transporters in chloride uptake in zebrafish (Danio rerio) larvae. *The Journal of experimental biology*, 212(Pt 20), pp.3283–3295.

Benos, D.J., 1982. Amiloride: a molecular probe of sodium transport in tissues and cells. *The American journal of physiology*, 242(3), pp.C131–C145.

Boyle, D. et al., 2015. Mechanisms of Cl− uptake in rainbow trout: Cloning and expression of slc26a6, a prospective Cl−/HCO3− exchanger. *Comparative Biochemistry and Physiology Part A: Molecular & Integrative Physiology*, 180, pp.43–50.

Cai, W.-J. et al., 2011. Acidification of subsurface coastal waters enhanced by eutrophication. *Nature Geoscience*, 4(11), pp.766–770.

Caldeira, K., 2005. Ocean model predictions of chemistry changes from carbon dioxide emissions to the atmosphere and ocean. *Journal of Geophysical Research*, 110(C9), pp.1–12.

Caldeira, K. & Wickett, M.E., 2003. Oceanography: anthropogenic carbon and ocean pH. *Nature*, 425(6956), p.365.

Catches, J.S. et al., 2006. Na+/H+ antiporter, V-H+-ATPase and Na+/K+-ATPase immunolocalization in a marine teleost (Myoxocephalus octodecemspinosus). *The Journal of experimental biology*, 209(Pt 17), pp.3440–3447.

Chernova, M.N. et al., 2003. Acute regulation of the SLC26A3 congenital chloride diarrhoea anion exchanger (DRA) expressed in Xenopus oocytes. *The Journal of physiology*, 549(Pt 1), pp.3–19.

Claiborne, J., Edwards, S. & Morrison-Shetlar, A., 2002. Acid-base regulation in fishes: Cellular and molecular mechanisms. *Journal of Experimental Zoology*, 293(3), pp.302–319.

Claiborne, J.B. et al., 1999. A mechanism for branchial acid excretion in marine fish: identification of multiple Na+/H+ antiporter (NHE) isoforms in gills of two seawater teleosts. *The Journal of experimental biology*, 202(Pt 3), pp.315–324.

Claiborne, J.B. et al., 2008. Molecular detection and immunological localization of gill Na+/H+ exchanger in the dogfish (Squalus acanthias). *American journal of*

physiology. Regulatory, integrative and comparative physiology, 294(3), pp.R1092–R1102.

Claiborne, J.B., Edwards, S.L. & Morrison-Shetlar, A., 2002. Acid-base regulation in fishes: Cellular and molecular mechanisms. *Journal of Experimental Zoology*, 293(April), pp.302–319.

Cripps, I.L., Munday, P.L. & McCormick, M.I., 2011. Ocean acidification affects prey detection by a predatory reef fish. *PLoS ONE*, 6(7), pp.1–7.

Dallos, P. & Fakler, B., 2002. Prestin, a new type of motor protein. *Nature reviews. Molecular cell biology*, 3(2), pp.104–111.

Dixson, D.L., Munday, P.L. & Jones, G.P., 2010. Ocean acidification disrupts the innate ability of fish to detect predator olfactory cues. *Ecology Letters*, 13(1), pp.68–75.

Edwards, S.L. et al., 2001. Expression of Na+/H+ exchanger mRNA in the gills of the Atlantic hagfish (Myxine glutinosa) in response to metabolic acidosis. *Comparative Biochemistry and Physiology - A Molecular and Integrative Physiology*, 130(1), pp.81–91.

Edwards, S.L. et al., 2005. The effect of environmental hypercapnia and salinity on the expression of NHE-like isoforms in the gills of a euryhaline fish (Fundulus heteroclitus). *Journal of Experimental Zoology Part A: Comparative Experimental Biology*, 303(6), pp.464–475.

Esbaugh, A. et al., In Review. Respiratory plasticity is insufficient to alleviate blood acid-base disturbances after acclimation to ocean acidification in the estuarine red drum, Sciaenops ocellatus . *Journal of Comparative Physiology B*.

Esbaugh, A.J. et al., 2005. Cytoplasmic carbonic anhydrase isozymes in rainbow trout Oncorhynchus mykiss: comparative physiology and molecular evolution. *The Journal of experimental biology*, 208(Pt 10), pp.1951–1961.

Esbaugh, A.J., Heuer, R. & Grosell, M., 2012. Impacts of ocean acidification on respiratory gas exchange and acid-base balance in a marine teleost, Opsanus beta. *Journal of Comparative Physiology B: Biochemical, Systemic, and Environmental Physiology*, 182, pp.921–934.

Evans, D.H., Piermarini, P.M. & Choe, K.P., 2005. The Multifunctional Fish Gill : Dominant Site of Gas Exchange , Osmoregulation , Acid-Base Regulation , and Excretion of Nitrogenous Waste. *Physiol Rev*, 85, pp.97–177.

Feely, R. a. et al., 2010. The combined effects of ocean acidification, mixing, and respiration on pH and carbonate saturation in an urbanized estuary. *Estuarine, Coastal and Shelf Science*, 88(4), pp.442–449.

Ferrari, M.C.O. et al., 2012. Effects of ocean acidification on learning in coral reef fishes. *PLoS ONE*, 7(2), pp.1–10.

Georgalis, T., Gilmour, K.M., et al., 2006. Roles of cytosolic and membrane-bound carbonic anhydrase in renal control of acid-base balance in rainbow trout, Oncorhynchus mykiss. *American journal of physiology. Renal physiology*, 291(2), pp.F407–F421.

Georgalis, T., Perry, S.F. & Gilmour, K.M., 2006. The role of branchial carbonic anhydrase in acid-base regulation in rainbow trout (Oncorhynchus mykiss). *The Journal of experimental biology*, 209(Pt 3), pp.518–530.

Gilmour, K.M. et al., 2012. Compensatory regulation of acid-base balance during salinity transfer in rainbow trout (Oncorhynchus mykiss). *Journal of Comparative Physiology B: Biochemical, Systemic, and Environmental Physiology*, 182(2), pp.259–274.

Gilmour, K.M. & Perry, S.F., 2009. Carbonic anhydrase and acid-base regulation in fish. *The Journal of experimental biology*, 212(Pt 11), pp.1647–1661.

Gonzalez, A. et al., 2013. Evolutionary rescue: an emerging focus at the intersection between ecology and evolution. *Philosophical transactions of the Royal Society of London. Series B, Biological sciences*, 368(1610), pp.1–8.

Goss, G.G. et al., 1998. Gill morphology and acid-base regulation in freshwater fishes. *Comparative Biochemistry and Physiology - A Molecular and Integrative Physiology*, 119(1), pp.107–115.

Grosell, M., Mager, E.M., et al., 2009. High rates of HCO3- secretion and Cl- absorption against adverse gradients in the marine teleost intestine: the involvement of an electrogenic anion exchanger and H+-pump metabolon? *The Journal of experimental biology*, 212(Pt 11), pp.1684–1696.

Grosell, M., 2006. Intestinal anion exchange in marine fish osmoregulation. *The Journal of experimental biology*, 209(Pt 15), pp.2813–2827.

Grosell, M., Genz, J., et al., 2009. The involvement of H+-ATPase and carbonic anhydrase in intestinal HCO3- secretion in seawater-acclimated rainbow trout. *The Journal of experimental biology*, 212(Pt 12), pp.1940–1948.

Grosell, M. & Genz, J., 2006. Ouabain-sensitive bicarbonate secretion and acid absorption by the marine teleost fish intestine play a role in osmoregulation. *American journal of physiology. Regulatory, integrative and comparative physiology*, 291(4), pp.R1145–R1156.

Guffey, S., Esbaugh, A. & Grosell, M., 2011. Regulation of apical H+-ATPase activity and intestinal HCO3- secretion in marine fish osmoregulation. *American journal of physiology. Regulatory, integrative and comparative physiology*, 301, pp.1682–1691.

Guffey, S.C., Fliegel, L. & Goss, G.G., 2015. Cloning and characterization of Na+/H+ Exchanger isoforms NHE2 and NHE3 from the gill of Pacific dogfish Squalus suckleyi. *Comparative Biochemistry and Physiology Part B: Biochemistry and Molecular Biology*, 188, pp.46–53.

Haswell, M.S., Randall, D.J. & Perry, S.F., 1980. Fish gill carbonic anhydrase: acid-base regulation or salt transport? *The American journal of physiology*, 238(3), pp.R240–R245.

Heuer, R.M., Esbaugh, a J. & Grosell, M., 2012. Ocean acidification leads to counterproductive intestinal base loss in the Gulf toadfish (Opsanus beta). *Physiological and Biochemical Zoology* , 85, pp.450–459.

Hu, M.Y. et al., 2013. Development in a naturally acidified environment: Na+/H+-exchanger 3-based proton secretion leads to CO2 tolerance in cephalopod embryos. *Frontiers in zoology*, 10(1), pp.1–16.

Ishimatsu, A., Hayashi, M. & Kikkawa, T., 2008. Fishes in high-CO2, acidified oceans. *Marine Ecology Progress Series*, 373(1), pp.295–302.

Ivanis, G., Esbaugh, a J. & Perry, S.F., 2008. Branchial expression and localization of SLC9A2 and SLC9A3 sodium/hydrogen exchangers and their possible role in acid-base regulation in freshwater rainbow trout (Oncorhynchus mykiss). *The Journal of experimental biology*, 211, pp.2467–2477.

Kumai, Y. & Perry, S.F., 2011. Ammonia excretion via Rhcg1 facilitates Na+ uptake in larval zebrafish, Danio rerio, in acidic water. *AJP: Regulatory, Integrative and Comparative Physiology*, 301(August), pp.R1517–R1528.

Lin, H. et al., 1994. Immunolocalization of H+-ATPase in the gill epithelia of rainbow trout. *The Journal of experimental biology*, 195(1), pp.169–83.

Liu, S.-T. et al., 2013. Proton-facilitated ammonia excretion by ionocytes of medaka (Oryzias latipes) acclimated to seawater. *American Journal of Physiology. Regulatory, Integrative and Comparative Physiology*, 305(3), pp.R242–R251.

Loretz, C.A., 1995. Electrophysiology of ion transport in teleost intestinal cells. In *Fish Physiology*. pp. 25–99.

Marshall, W.M. & Grosell, M., 2005. Ion Transport, Osmoregulation, and Acid-Base Balance. In *Physiology of Fishes*. pp. 177–203.

Marshall, W.S. & Grosell, M., 2005. Ion Osmoregulation , and Acid – Base Balance. *The Physiology of Fishes*, pp.177–230.

Matlock, G.C., 1987. The Life History of Red Drum. *Red Drum Aquaculture*, pp.1–21.

Meehl, G. et al., 2007. Global Climate Predictions. In *Climate Change 2007: The Physical Science Basis*. Cambridge, UK: Cambridge University Press, pp. 747–846.

Mount, D.B. & Romero, M.F., 2004. The SLC26 gene family of multifunctional anion exchangers. *Pflugers Archiv European Journal of Physiology*, 447(5), pp.710–721.

Munday, P.L. et al., 2009. Ocean acidification impairs olfactory discrimination and homing ability of a marine fish. *Proceedings of the National Academy of Sciences of the United States of America*, 106, pp.1848–1852.

Munday, P.L. et al., 2010. Replenishment of fish populations is threatened by ocean acidification. *Proceedings of the National Academy of Sciences of the United States of America*, 107(29), pp.12930–12934.

Nilsson, G.E. et al., 2012. Near-future carbon dioxide levels alter fish behaviour by interfering with neurotransmitter function. *Nature Climate Change*, 2(3), pp.201–204.

Orlowski, J. & Grinstein, S., 2004. Diversity of the mammalian sodium/proton exchanger SLC9 gene family. *Pflugers Archiv European Journal of Physiology*, 447(5), pp.549–565.

Orr, J.C. et al., 2005. Anthropogenic ocean acidification over the twenty-first century and its impact on calcifying organisms. *Nature*, 437(7059), pp.681–686.

Parks, S.K., Tresguerres, M. & Goss, G.G., 2009. Cellular mechanisms of Cl- transport in trout gill mitochondrion-rich cells. *American journal of physiology. Regulatory, integrative and comparative physiology*, 296(4), pp.R1161–R1169.

Parks, S.K., Tresguerres, M. & Goss, G.G., 2008. Theoretical considerations underlying Na+ uptake mechanisms in freshwater fishes. *Comparative Biochemistry and Physiology - C Toxicology and Pharmacology*, 148(4), pp.411–418.

Perry, S.F. et al., 2010. Acid-base regulation in the plainfin midshipman (Porichthys notatus): An aglomerular marine teleost. *Journal of Comparative Physiology B: Biochemical, Systemic, and Environmental Physiology*, 180, pp.1213–1225.

Perry, S.F. et al., 2009. Gas Transport and Gill Function in Water-Breathing Fish. In *Cardio-respiratory Control in Vertebrates: Comparative and Evolutionary Aspects*. Berlin: Springer Verlag, pp. 5–31.

Perry, S.F. & Gilmour, K.M., 2006. Acid-base balance and CO2 excretion in fish: Unanswered questions and emerging models. *Respiratory Physiology and Neurobiology*, 154, pp.199–215.

Pfaffl, M., 2004. Quantification strategies in real-time PCR Michael W . Pfaffl. *A-Z of quantitative PCR*, pp.87–112.

Pfister, C. a. et al., 2014. Detecting the Unexpected: A Research Framework for Ocean Acidification. *Environmental Science & Technology*, 48(SEPTEMBER), pp.9982–9994.

Raven, J. et al., 2005. Ocean acidification due to increasing atmospheric carbon dioxide. *Coral Reefs*, 5(June), pp.1–59.

Reilly, B.D. et al., 2011. Branchial osmoregulation in the euryhaline bull shark, Carcharhinus leucas: a molecular analysis of ion transporters. *The Journal of experimental biology*, 214(Pt 17), pp.2883–2895.

Riou, V. et al., 2012. Impact of environmental DDT concentrations on gill adaptation to increased salinity in the tilapia Sarotherodon melanotheron. *Comparative Biochemistry and Physiology - C Toxicology and Pharmacology*, 156(1), pp.7–16.

Roa, J.N., Munévar, C.L. & Tresguerres, M., 2014. Feeding induces translocation of vacuolar proton ATPase and pendrin to the membrane of leopard shark (Triakis semifasciata) mitochondrion-rich gill cells. *Comparative Biochemistry and Physiology -Part A : Molecular and Integrative Physiology*, 174, pp.29–37.

Rooker, J. & Holt, S., 1997. Utilization of subtropical seagrass meadows by newly settled red drum Sciaenops ocellatus:patterns of distribution and growth . *Marine Ecology Progress Series*, 158(August), pp.139–149.

Schaechinger, T.J. & Oliver, D., 2007. Nonmammalian orthologs of prestin (SLC26A5) are electrogenic divalent/chloride anion exchangers. *Proceedings of the National Academy of Sciences of the United States of America*, 104(18), pp.7693–7698.

Scott, G.R. et al., 2005. Gene expression after freshwater transfer in gills and opercular epithelia of killifish: insight into divergent mechanisms of ion transport. *The Journal of experimental biology*, 208(Pt 14), pp.2719–2729.

Simpson, S.D. et al., 2011. Ocean acidification erodes crucial auditory behaviour in a marine fish. *Biology Letters*, 7(6), pp.917–920.

Strobel, A. et al., 2012. Metabolic shifts in the Antarctic fish Notothenia rossii in response to rising temperature and PCO2. *Frontiers in Zoology*, 9(28), pp.1–15.

Stunz, G.W., Minello, T.J. & Levin, P.S., 2002. Growth of newly settled red drum Sciaenops ocellatus in different estuarine habitat types. *Marine Ecology Progress Series*, 238(Fuiman 1994), pp.227–236.

Sucré, E. et al., 2010. Embryonic occurrence of ionocytes in the sea bass Dicentrarchus labrax. *Cell and Tissue Research*, 339(3), pp.543–550.

Tan, X. et al., 2011. From zebrafish to mammal: functional evolution of prestin, the motor protein of cochlear outer hair cells. *Journal of neurophysiology*, 105, pp.36–44.

Taylor, J.R., Mager, E.M. & Grosell, M., 2010. Basolateral NBCe1 plays a rate-limiting role in transepithelial intestinal HCO3- secretion, contributing to marine fish osmoregulation. *The Journal of experimental biology*, 213(3), pp.459–468.

Tresguerres, M., Parks, S.K., et al., 2007. V-H+ -ATPase translocation during blood alkalosis in dogfish gills: interaction with carbonic anhydrase and involvement in the postfeeding alkaline tide. *American journal of physiology. Regulatory, integrative and comparative physiology*, 292(5), pp.R2012–R2019.

Tresguerres, M., Parks, S.K. & Goss, G.G., 2007. Recovery from blood alkalosis in the Pacific hagfish (Eptatretus stoutii): Involvement of gill V-H+-ATPase and Na+/K+-ATPase. *Comparative Biochemistry and Physiology - A Molecular and Integrative Physiology*, 148(1 SPEC. ISS.), pp.133–141.

Tseng, Y.-C. et al., 2007. Glycogen phosphorylase in glycogen-rich cells is involved in the energy supply for ion regulation in fish gill epithelia. *American journal of physiology. Regulatory, integrative and comparative physiology*, 293(1), pp.R482–R491.

Verdouw, H., van Echted, C.J.A. & Dekkers, E.M.J., 1978. Ammonia determination based on indophenol formation with sodium salicylate. *Water Res*, 12, pp.399–402.

Watson, C.J., Nordi, W.M. & Esbaugh, A.J., 2014. Osmoregulation and branchial plasticity after acute freshwater transfer in red drum, Sciaenops ocellatus. *Comparative Biochemistry and Physiology Part A: Molecular & Integrative Physiology*, 178, pp.82–89.

Vita

Elizabeth Ann Brown was born in San Antonio, Texas. After completing her high school degree at Independence High School in Thompson's Station, Tennessee in 2008, she attended the University of Texas at San Antonio for two years. She then transferred to Shepherd University in Shepherdstown, West Virginia where she received a Bachelor of Science in Biology with a concentration in Ecological Sciences in 2012. She attended the University of Texas Health Science Center at San Antonio in 2013 where she earned her certification as an EMT-Basic. In 2013 she began studying at the University of Texas at Austin's Marine Science Institute in Port Aransas where she received her Master of Science in Marine Science in 2015.

Email address: elizabeth.brown@utexas.edu

This thesis was typed by Elizabeth Ann Brown.